Transparent Boundary Conditions for Wave Propagation in Fractal Trees: Approximation by Local Operators

Patrick Joly, Maryna Kachanovska

TRANSPARENT BOUNDARY CONDITIONS FOR WAVE PROPAGATION IN FRACTAL TREES: APPROXIMATION BY LOCAL OPERATORS

PATRICK JOLY AND MARYNA KACHANOVSKA

Abstract. This work is dedicated to the construction and analysis of high-order transparent boundary conditions for the weighted wave equation on a fractal tree, which models sound propagation inside human lungs. This article follows the works [10, 9], aimed at the analysis and numerical treatment of the model, as well as the construction of low-order and exact discrete boundary conditions. The method suggested in this article is based on the truncation of the meromorphic series that approximate the symbol of the Dirichlet-to-Neumann operator, similarly to the absorbing boundary conditions of B. Engquist and A. Majda. We analyze its stability, convergence and complexity. The error analysis is largely based on spectral estimates of the underlying weighted Laplacian.

Numerical results confirm the efficiency of the method.

1. Introduction

Modelling sound propagation in a human lung is important for medical diagnostics, see e.g. the Audible Human Project [1], [19] and references therein. Because the physical phenomenon of wave propagation in a lung is highly complex and multi-scale, its computational tractability relies on the use of simplified models. One of such models is based on the geometric representation of a bronchiolar tree as a self-similar network of tubes, see [17, 8, 18]. An asymptotic analysis of the 3D wave equation posed on such a network, with respect to the thickness of the tubes tending to zero, leads to a weighed 1D wave equation on a self-similar tree, see [11, 20]. A complete mathematical analysis of this model was performed in [10].

Because such a tree has an infinite number of edges, to perform any kind of numerical simulations, we need to be able to truncate the computational domain. This is classically done via introducing absorbing boundary conditions, which, in turn are based on the approximation of the Dirichlet-to-Neumann (DtN) operator. The principal difficulty lies in its time-domain non-locality. One of the methods for the approximation of the DtN, in the spirit of the convolution quadrature approach, was proposed in [9]; however, it suffers from a rather high computational costs on long times. In this work we would propose an alternative method to approximate the DtN, based on the classical ideas of Engquist and Majda [6], namely, replace the frequency-domain DtN by a rational function.

Compared to the classical case of the free wave propagation, there are multiple additional difficulties associated to the model we study. In particular, it describes the wave propagation in heterogeneous media, and exhibits multi-scale phenomena.

2010 *Mathematics Subject Classification.* 65M12, 65M15, 35P20, 28A80,35L05.

As a result, no closed form expression for the Green function is available. Nonetheless, in [10] it was shown that the symbol of the DtN operator is a meromorphic function, which satisfies a certain non-linear equation. Truncating the respective elementary fraction expansion at first poles results in an approximation of the symbol of the DtN operator that can be realized via local operators in the time domain. We prove the stability of such boundary conditions, as well as perform the error analysis for them; moreover, we demonstrate how to choose the number of poles to achieve a desired accuracy. This analysis is largely based on the asymptotic estimates on the eigenvalues of the underlying weighted Laplacian.

This article is organized as follows. In Section 2 we review the notation and state the problem. In Section 3 we propose the approximation of the transparent boundary conditions, present the stability and error analysis. We will demonstrate that the respective error is controlled by a remainder of convergent series, which depends on the eigenvalues and normal derivatives of the corresponding eigenfunctions. Section 4 is dedicated to the analysis of the behaviour of this remainder and, in particular, to its control. In Section 5 we present more numerical aspects of the method, namely, its stable discretization and algorithm for computing the approximation of the DtN. In the end of this section some numerical results are provided. Finally, Section 6 is dedicated to the conclusions and open problems.

2. Problem setting

The content of this section is not new, and presents a shortened description of the corresponding section in [9].

2.1. **Notation.** Let $\mathcal{T}$ be an infinite (in terms of the number of edges) p-adic tree [10, Definiton 2.1]. We will call a generation $\mathcal{G}^i$ a set of edges constructed as follows: $\mathcal{G}^0$ contains a root edge only; $\mathcal{G}^{n+1}$ consists of all children edges of all edges $\Sigma \in \mathcal{G}^n$. The p^n edges belonging to $\mathcal{G}^n$ will be denoted by

$$\Sigma_{n,k},\ k = 0, \dots, p^n - 1.$$

The edge $\Sigma_{n,k}$ has p children

$$\Sigma_{n+1,pk+j}, \qquad j = 0, \dots, p-1. \tag{2.1}$$

Besides edges, we will consider the vertices of the tree; the root vertex of $\mathcal{T}$ will be denoted by M^*. An edge $\Sigma_{n,k}$ can be identified with a segment $[A_{n,k}, B_{n,k}]$. One of the vertices $A_{n,k}$, $M_{n,k}$ defines the edge $\Sigma_{n,k}$ uniquely; we will denote this vertex by $M_{n,k}$ (see Figure 1). Mathematically, it can be defined as follows. First of all, for a vertex M, we introduce $d(M)$ be the distance between M^* and M (defined as the sum of the respective edge lengths). Then

$$M_{n,k} = \operatorname{argmax}(d(A_{n,k}), d(B_{n,k})).$$

With each edge $\Sigma_{n,k}$ we will associate two positive quantities: its length $\ell_{n,k}$ and a constant weight $\mu_{n,k}$. Without loss of generality, we will assume that $\mu_{0,0} = 1$.

In what follows, we will consider self-similar (fractal) trees, see [10, Definition 2.3]. Namely, let $\boldsymbol{\alpha} = (\alpha_0, \dots, \alpha_{p-1})$ and $\boldsymbol{\mu} = (\mu_0, \dots, \mu_{p-1})$. Then the length/weight of the edge $\Sigma_{n+1,pk+j}$ is related to the length/weight of its parent edge $\Sigma_{n,k}$:

$$\ell_{n+1,pk+j} = \alpha_j \ell_{n,k}, \qquad \mu_{n+1,pk+j} = \mu_j \mu_{n,k}, \qquad j = 0, \dots, p-1.$$

This is illustrated in Figure 1.

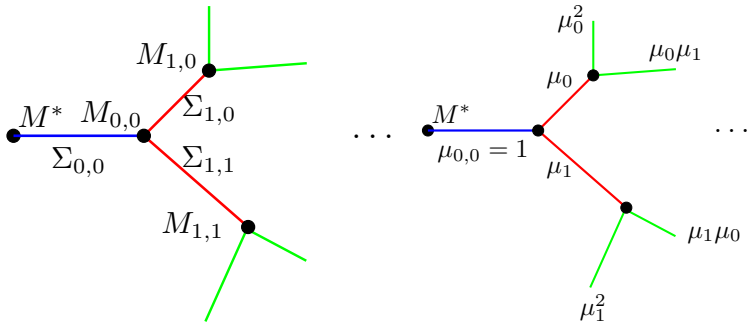

FIGURE 1. Left: A self-similar p-adic ($p = 2$) infinite tree. In blue we mark the edges that belong to $\mathcal{G}^0$, in red the edges of $\mathcal{G}^1$, in green the edges of $\mathcal{G}^2$. Right: Distribution of weights on the edges of a 2-adic infinite self-similar tree.

By $\mathcal{T}^m$ we denote the subtree of $\mathcal{T}$ containing the first m generations, i.e. $\bigcup_{\ell=0}^{m} \mathcal{G}^\ell$.

We will assume that $|\boldsymbol{\alpha}|_\infty < 1$. Finally, we will call a weighted tree $\mathcal{T}$ a reference tree if the length of its root edge $\ell_{0,0} = 1$.

2.2. **The weighted wave equation on fractal trees.** In order to introduce the model under consideration, let us first define a parameterization of an edge $\Sigma_{n,j}$ by an abscissa $s_{n,j} \in [a_{n,j}, b_{n,j}]$, $a_{n,j}$, $b_{n,j} \in \mathbb{R}$. Provided that $\Sigma_{n,j}$ is associated with the segment $[M^*_{n,j}, M_{n,j}]$, where $M^*_{n,j}$, $M_{n,j}$ are vertices of $\mathcal{T}$, this parametrization satisfies

$$[M^*_{n,j},\, M_{n,j}] \equiv \{M \in \mathbb{R}^d :\, M = M^*_{n,j} + (M_{n,j} - M^*_{n,j})(s_{n,j} - a_{n,j})(b_{n,j} - a_{n,j})^{-1}\}.$$

Let s be an abscissa on the tree $\mathcal{T}$ (for each edge $\Sigma_{n,j}$ defined as above); formally, let us define the weight function $\mu(s)$ on $\mathcal{T}$ as follows: $\mu(s) = \mu_{n,j}$, $s \in \Sigma_{n,j}$ (with an obvious abuse of notation). We look for an acoustic pressure $u(s,t)$ satisfying

$$\mu \partial_t^2 u - \partial_s(\mu \partial_s u) = f(s,t), \tag{2.2}$$

(here f is a source term), with vanishing initial conditions and a boundary condition $u(M^*, t) = 0$. Additionally, we need to define the BCs at the 'infinite', fractal boundary of the tree, which we will formalize in Section 2.3. Let us first explain the meaning of (2.2). With $u_{n,j} = u|_{\Sigma_{n,j}}$, (2.2) is a shortened notation for

$$\partial_t^2 u_{n,j} - \partial_s^2 u_{n,j} = f_{n,j} \quad \text{on } \Sigma_{n,j}, \qquad j = 0, \dots p^n - 1, \quad n \geq 0, \tag{2.3}$$

$$u(.,0) = \partial_t u(.,0) = 0, \quad u(M^*, t) = 0, \tag{2.4}$$

with u satisfying continuity ($\mathcal{C}$) and Kirchoff ($\mathcal{K}$) conditions at all the vertices, see (2.1) (with an obvious abuse of notation)

$$(\mathcal{C}) \quad u_{n,j}(M_{n,j}, t) = u_{n+1,pj+k}(M_{n,j}, t), \quad k = 0, \dots, p-1,$$

$$(\mathcal{K}) \quad \partial_s u_{n,j}(M_{n,j}, t) = \sum_{k=0}^{p-1} \mu_k\, \partial_s u_{n+1,pj+k}(M_{n,j}, t), \qquad j = 0, \dots p^n - 1,\ n \geq 0.$$

2.3. **Dirichlet and Neumann BVPs for (2.2).** To provide a rigorous mathematical formulation of the problem (2.3, 2.4, $\mathcal{C}$, $\mathcal{K}$), we need to equip it with auxiliary boundary conditions at the 'infinite' boundary of the tree. This is done variationally, via the associated Sobolev spaces.

2.3.1. *Sobolev Spaces.* For a function $v : \mathcal{T} \to \mathbb{C}$, let

$$\int_{\mathcal{T}} \mu v := \sum_{n=0}^{\infty} \sum_{k=0}^{p^n-1} \int_{\Sigma_{n,k}} \mu_{n,k} v(s) ds \tag{2.5}$$

Let $C(\mathcal{T})$ be a space of continuous functions on $\mathcal{T}$, and

$$C_0(\mathcal{T}) := \{v \in C(\mathcal{T}) : \quad v = 0 \text{ on } \mathcal{T} \setminus \mathcal{T}^m, \quad \text{for some } m \in \mathbb{N}\}.$$

Let us introduce the following three spaces. First of all,

$$\mathrm{L}^2_\mu(\mathcal{T}) = \{v : \ v|_{\Sigma_{n,j}} \in \mathrm{L}^2(\Sigma_{n,j}),\ \|v\|_{\mathrm{L}^2_\mu(\mathcal{T})} < \infty\}, \quad \|v\|^2_{\mathrm{L}^2_\mu(\mathcal{T})} = \|v\|^2 = \int_{\mathcal{T}} \mu |v|^2.$$

We will denote by $(.,.)$ an associated scalar product. The weighted Sobolev space H^1_μ is defined in a natural way:

$$\mathrm{H}^1_\mu(\mathcal{T}) := \{v \in C(\mathcal{T}) \cap \mathrm{L}^2_\mu(\mathcal{T}) : \|\partial_s v\| < \infty\}, \quad \|v\|^2_{\mathrm{H}^1_\mu(\mathcal{T})} = \|v\|^2 + \|\partial_s v\|^2.$$

The remaining space is an analogue of the classical H^1_0-space:

$$\mathrm{H}^1_{\mu,0}(\mathcal{T}) := \overline{C_0(\mathcal{T}) \cap \mathrm{H}^1_\mu(\mathcal{T})}^{\|.\|_{\mathrm{H}^1_\mu(\mathcal{T})}}.$$

Analogously, we define the corresponding spaces on a truncated tree $\mathcal{T}^m$. The associated L^2_μ-scalar product will be denoted by $(.,.)_{\mathcal{T}^m}$.

2.3.2. *The BVP problems.* To formulate Dirichlet/Neumann problems for (2.2), let us introduce auxiliary spaces (for brevity denoted in what follows by $V_\mathfrak{n}$, $V_\mathfrak{d}$):

$$V_\mathfrak{n}(\mathcal{T}) = \{v \in \mathrm{H}^1_\mu(\mathcal{T}) : \ v(M^*) = 0\},\ V_\mathfrak{d}(\mathcal{T}) = \{v \in \mathrm{H}^1_{\mu,0}(\mathcal{T}) : \ v(M^*) = 0\}.$$

Let $T > 0$ denote the final time.

Definition 2.1 (Time-domain Neumann problem)**.** Find

$$u_\mathfrak{n} \in C([0,T]; V_\mathfrak{n}) \cap C^1([0,T]; \mathrm{L}^2_\mu(\mathcal{T})),\ \text{s.t. } u_\mathfrak{n}(.,0) = \partial_t u_\mathfrak{n}(.,0) = 0,\ \text{and}$$

$$\int_{\mathcal{T}} \mu \frac{d^2}{dt^2} u_\mathfrak{n}\, v + \int_{\mathcal{T}} \mu \partial_s u_\mathfrak{n} \partial_s v = \int_{\mathcal{T}} \mu f v, \qquad \text{for all } v \in V_\mathfrak{n}. \tag{N}$$

Definition 2.2 (Time-domain Dirichlet problem)**.** Find

$$u_\mathfrak{d} \in C([0,T]; V_\mathfrak{d}) \cap C^1([0,T]; \mathrm{L}^2_\mu(\mathcal{T})),\ \text{s.t. } u_\mathfrak{d}(.,0) = \partial_t u_\mathfrak{d}(.,0) = 0,\ \text{and}$$

$$\int_{\mathcal{T}} \mu \frac{d^2}{dt^2} u_\mathfrak{d}\, v + \int_{\mathcal{T}} \mu \partial_s u_\mathfrak{d} \partial_s v = \int_{\mathcal{T}} \mu f v, \qquad \text{for all } v \in V_\mathfrak{d}. \tag{D}$$

The above problems are well-posed and stable whenever $f \in L^1(0,\, T; \mathrm{L}^2_\mu(\mathcal{T}))$, cf. [9, Theorem 1]. It appears that in some cases the solutions to (N) and (D) coincide. To explain this result in more detail, let us introduce

$$\langle \boldsymbol{\mu}\boldsymbol{\alpha}\rangle := \sum_{i=0}^{p-1} \mu_i \alpha_i, \qquad \left\langle \frac{\boldsymbol{\mu}}{\boldsymbol{\alpha}} \right\rangle := \sum_{i=0}^{p-1} \frac{\mu_i}{\alpha_i}.$$

Because $|\boldsymbol{\alpha}|_\infty < 1$, $\langle \boldsymbol{\mu}\boldsymbol{\alpha}\rangle < \left\langle \frac{\boldsymbol{\mu}}{\boldsymbol{\alpha}} \right\rangle$.

Theorem 2.3 ([10])**.** *If* $\langle \boldsymbol{\mu}\boldsymbol{\alpha}\rangle \geq 1$ *or* $\left\langle \frac{\boldsymbol{\mu}}{\boldsymbol{\alpha}} \right\rangle \leq 1$*, the spaces* $\mathrm{H}^1_{\mu,0}(\mathcal{T})$ *and* $\mathrm{H}^1_\mu(\mathcal{T})$ *coincide, and thus* $u_{\mathfrak{n}} = u_{\mathfrak{d}}$*. Otherwise,* $\mathrm{H}^1_{\mu,0}(\mathcal{T}) \subsetneq \mathrm{H}^1_\mu(\mathcal{T})$*, and* $u_{\mathfrak{n}} \neq u_{\mathfrak{d}}$*.*

The next result clarifies the question of the embedding of $\mathrm{H}^1_\mu(\mathcal{T})$ into $\mathrm{L}^2_\mu(\mathcal{T})$.

Theorem 2.4. *The embedding of* $\mathrm{H}^1_\mu(\mathcal{T})$ *into* $\mathrm{L}^2_\mu(\mathcal{T})$ *is compact.*

2.4. **Transparent Boundary Conditions.** The construction of transparent boundary conditions for the Dirichlet and Neumann problems is based on the results of [10] and [9]. Let us fix $m \geq 1$. We will assume that the source term is compactly supported in $\mathcal{T}^{m-1}$ for all $t \geq 0$.

2.4.1. *Notation.* Let $\mathbf{V}_\mu(\mathcal{T}^m) := \{v \in \mathrm{H}^1_\mu(\mathcal{T}^m) : v(M^*) = 0\}$. For $v \in \mathbf{V}_\mu(\mathcal{T}^m)$ we define a partial trace operator

$$\boldsymbol{\gamma}_m : \quad \mathbf{V}_\mu(\mathcal{T}^m) \to \mathbb{R}^{p^m}, \qquad \boldsymbol{\gamma}_m v = \left(v(M_{m,0}), \dots, v(M_{m,p^m-1})\right).$$

Let us additionally introduce, for $g \in \mathbf{V}_\mu(\mathcal{T}^m)$ and $f_1,\, f_2 : \mathbb{R} \to \mathbb{R}$,

$$\int_{\Gamma_m} f_1(\boldsymbol{\mu}) f_2(\boldsymbol{\alpha}) \boldsymbol{g} := \sum_{j=0}^{p^m-1} f_1(\mu_{m,j}) f_2(\alpha_{m,j}) g(M_{m,j}). \tag{2.6}$$

2.4.2. *Transparent boundary conditions.* To truncate the computational domain to the tree $\mathcal{T}^m$, we will impose at its boundary the transparent BCs:

$$-\mu_{m,j}\partial_s u_{m,j}(M_{m,j}, t) = \mathcal{B}^{\mathfrak{a}}_{m,j}(\partial_t) u_{m,j}(M_{m,j}, t), \quad j = 0, \dots, p^m - 1, \tag{2.7}$$

where $\mathfrak{a} \in \{\mathfrak{d}, \mathfrak{n}\}$, $\mathcal{B}^{\mathfrak{a}}_{m,j}(\partial_t)$ is an exact DtN operator associated to the point $M_{m,j}$. It is a convolution operator whose convolution kernel is not known in explicit form, but which admits a tractable characterization in terms of a so-called reference DtN. Reference DtN operator. Provided $g \in H^1([0,T])$, s.t. $g|_{t=0} = 0$, let us define the reference DtN operator on the **reference** tree $\mathcal{T}$ (according to [10]) as follows:

$$\boldsymbol{\Lambda}_{\mathfrak{a}}(\partial_t) g(t) = -\partial_s u^{\mathfrak{a}}_g(M^*, t),$$

where (see [15] for the regularity results stated below)

(1) the function $u^{\mathfrak{d}}_g \in C([0,T]; \mathrm{H}^1_{\mu,0}(\mathcal{T})) \cap C^1([0,T]; \mathrm{L}^2_\mu(\mathcal{T}))$ solves

$$\begin{aligned} &\int_{\mathcal{T}} \mu \frac{d^2}{dt^2} u^{\mathfrak{d}}_g \, v + \int_{\mathcal{T}} \mu \partial_s u^{\mathfrak{d}}_g \, \partial_s v = 0, \qquad \text{for all } v \in V_{\mathfrak{d}}, \\ &u^{\mathfrak{d}}_g(M^*, t) = g(t), \quad u^{\mathfrak{d}}_g(., 0) = \partial_t u^{\mathfrak{d}}_g(., 0) = 0. \end{aligned} \tag{2.8}$$

(2) the function $u^{\mathfrak{n}}_g \in C([0,T]; \mathrm{H}^1_\mu(\mathcal{T})) \cap C^1([0,T]; \mathrm{L}^2_\mu(\mathcal{T}))$ solves (2.8) where $u^{\mathfrak{d}}_g$ is substituted by $u^{\mathfrak{n}}_g$ and $V_{\mathfrak{d}}$ by $V_{\mathfrak{n}}$.

It can be shown that $\mathbf{\Lambda}_{\mathfrak{a}}(\partial_t)$ is a convolution operator, i.e.

$$\mathbf{\Lambda}_{\mathfrak{a}}(\partial_t)g(t) = \int_0^t \lambda_{\mathfrak{a}}(t-\tau)g(\tau)d\tau.$$

To define the symbol of $\mathbf{\Lambda}_{\mathfrak{a}}$, we will use the following convention for the Fourier-Laplace transform of a causal tempered distribution λ:

$$\hat{\lambda}(\omega) = (\mathcal{F}\lambda)(\omega) = \int_0^\infty \mathrm{e}^{i\omega t}\lambda(t)dt, \qquad \omega \in \mathbb{C}.$$

The symbol of the convolution operator $\mathbf{\Lambda}_{\mathfrak{a}}$ will be denoted by $\mathbf{\Lambda}_{\mathfrak{a}}(\omega) = (\mathcal{F}\lambda_{\mathfrak{a}})(\omega)$.

The symbol of the reference DtN can be computed for any $\omega \in \mathbb{C}^+ = \{z \in \mathbb{C} : \operatorname{Im} z > 0\}$, as shown in [9, Section 4].

Transparent BCs via the reference DtN and the coupled problem. The operator $\mathcal{B}^{\mathfrak{a}}_{m,j}(\partial_t)$ can be expressed as the following linear combination, cf. [10, 9]:

$$\mathcal{B}^{\mathfrak{a}}_{m,j}(\partial_t) = \mu_{m,j}\alpha_{m,j}^{-1}\sum_{k=0}^{p-1}\frac{\mu_k}{\alpha_k}\mathbf{\Lambda}_{\mathfrak{a}}(\alpha_k\alpha_{m,j}\partial_t). \tag{2.9}$$

Recall that $\alpha_{m,j}$ is the length of the branch $\Sigma_{m,j}$. The above representation follows from (2.7), Kirchoff conditions and a simple scaling argument. In conclusion, the problem of approximating $\mathcal{B}^{\mathfrak{a}}_{m,j}$ reduces to the problem of approximating $\mathbf{\Lambda}_{\mathfrak{a}}(\partial_t)$.

To formulate the coupled problem, let us introduce the following notation

$$\mathcal{B}^{\mathfrak{a}}_{m}(\partial_t) = \operatorname{diag}\left(\mathcal{B}^{\mathfrak{a}}_{m,0}(\partial_t), \dots, \mathcal{B}^{\mathfrak{a}}_{m,p^m-1}(\partial_t)\right). \tag{2.10}$$

With the above and (2.6), the variational formulation with the transparent BCs reads:

$$\text{find } u_{\mathfrak{a}} \in C([0,\,T];\boldsymbol{V}_\mu(\mathcal{T}^m)) \cap C^1([0,\,T];\mathrm{L}^2_\mu(\mathcal{T}^m)),$$

s.t. $u_{\mathfrak{a}}(.,0) = \partial_t u_{\mathfrak{a}}(.,0) = 0$ and, for all $v \in \boldsymbol{V}_\mu(\mathcal{T}^m)$,

$$(\partial_t^2 u_{\mathfrak{a}}, v)_{\mathcal{T}^m} + (\partial_s u_{\mathfrak{a}}, \partial_s v)_{\mathcal{T}^m} + \int_{\Gamma_m} \mathcal{B}_{m,\mathfrak{a}}(\partial_t)\boldsymbol{u}_{\mathfrak{a}}\,\boldsymbol{v} = (f, v)_{\mathcal{T}^m},\ \mathfrak{a} \in \{\mathfrak{d}, \mathfrak{n}\}. \tag{2.11}$$

3. Approximation of transparent boundary conditions

This section is organized as follows: in Section 3.1 we provide an approximation of the reference DtN and analyze its error. Section 3.2 deals with the stability and error analysis of the respective coupled formulation.

3.1. **Principal idea: truncated reference DtN operator.**

3.1.1. *One realization of the reference DtN operator in the time domain.* The main idea of our approach relies on the representation of the symbol of the DtN operator as a meromorphic series. Let us provide more details about this representation. Given a symmetric sesquilinear form

$$a(u,v) = \sum_{n=0}^{\infty}\sum_{k=0}^{p^n-1}\int_{\Sigma_{n,k}} \mu_{n,k}\partial_s u\,\partial_s\overline{v}ds, \tag{3.1}$$

let us define the following operators:

$$\mathcal{A}_{\mathfrak{a}}: \qquad D(\mathcal{A}_{\mathfrak{a}}) \to \mathrm{L}^2_\mu(\mathcal{T}), \qquad (A_{\mathfrak{a}}u, v) = a(u, v), \tag{3.2}$$

$$D(\mathcal{A}_{\mathfrak{a}}) = \{v \in V_{\mathfrak{a}} : \ |a(v, g)| < C(v)\|g\|_{\mathrm{L}^2_\mu(\mathcal{T})}, \text{ for all } g \in V_{\mathfrak{a}}\}. \tag{3.3}$$

From Theorem 2.4 it follows that the spectrum of these operators is a pure point spectrum. We define the eigenvalues and normalized eigenfunctions as

$$\mathcal{A}_{\mathfrak{a}}\varphi_{\mathfrak{a},n} = \omega^2_{\mathfrak{a},n}\varphi_{\mathfrak{a},n}, \qquad \|\varphi_{\mathfrak{a},n}\|_{\mathrm{L}^2_\mu(\mathcal{T})} = 1, \qquad 0 < \omega^2_{\mathfrak{a},1} \le \omega^2_{\mathfrak{a},2} \le \ldots \to +\infty, \tag{3.4}$$

The fact that the eigenvalues do not vanish was shown in [10, Remark 1.20].

Theorem 3.1 (Proposition 1.23, discussion after (144) in [10])**.** *The symbol of the reference DtN $\mathbf{\Lambda}_{\mathfrak{a}}$, $\mathfrak{a} \in \{\mathfrak{n}, \mathfrak{d}\}$ satisfies*

$$\mathbf{\Lambda}_{\mathfrak{a}}(\omega) = \mathbf{\Lambda}_{\mathfrak{a}}(0) - \sum_{n=1}^{+\infty} \frac{a_{\mathfrak{a},n}\omega^2}{(\omega_{\mathfrak{a},n})^2 - \omega^2}, \quad a_{\mathfrak{a},n} = \omega^{-2}_{\mathfrak{a},n}\left(\partial_s\varphi_{\mathfrak{a},n}(M^*)\right)^2. \tag{3.5}$$

The above series converges uniformly on compact subsets of $\mathbb{C}$ that do not contain the poles of $\mathbf{\Lambda}_{\mathfrak{a}}$. Moreover, $\mathbf{\Lambda}_{\mathfrak{a}}(0) \ge 0$.

The values of $\mathbf{\Lambda}_{\mathfrak{a}}(0)$ will play a rather important role in the error analysis; hence we summarize them below, see also Theorem 2.3.

Proposition 3.2 (Lemma 5.5, Corollary 5.6 in [10])**.** *The values of $\mathbf{\Lambda}_{\mathfrak{a}}(0)$ are as follows:*

- *if $\left\langle \frac{\boldsymbol{\mu}}{\boldsymbol{\alpha}} \right\rangle \le 1$, $\mathbf{\Lambda}_{\mathfrak{d}} \equiv \mathbf{\Lambda}_{\mathfrak{n}}$ and $\mathbf{\Lambda}_{\mathfrak{d}}(0) = 0$.*
- *let $\left\langle \frac{\boldsymbol{\mu}}{\boldsymbol{\alpha}} \right\rangle > 1$ and $\langle \boldsymbol{\mu}\boldsymbol{\alpha} \rangle < 1$. Then $\mathbf{\Lambda}_{\mathfrak{d}}(0) = 1 - \left\langle \frac{\boldsymbol{\mu}}{\boldsymbol{\alpha}} \right\rangle^{-1}$ and $\mathbf{\Lambda}_{\mathfrak{n}}(0) = 0$.*
- *if $\langle \boldsymbol{\mu}\boldsymbol{\alpha} \rangle \ge 1$, $\mathbf{\Lambda}_{\mathfrak{d}} \equiv \mathbf{\Lambda}_{\mathfrak{n}}$ and $\mathbf{\Lambda}_{\mathfrak{d}}(0) = 1 - \left\langle \frac{\boldsymbol{\mu}}{\boldsymbol{\alpha}} \right\rangle^{-1}$.*

For brevity, for the moment we will omit the index $\mathfrak{a}$, since the results of this section are valid both for the Dirichlet and Neumann problems.

Theorem 3.1 provides a convenient way to realize the DtN operator in the time domain. In particular, the symbol $\frac{i\omega}{\omega^2_\ell - \omega^2}$ corresponds to the following operator:

$$\hat{\lambda} = \frac{i\omega}{\omega^2_\ell - \omega^2}\hat{g} \iff \partial^2_t\lambda + \omega^2_\ell\lambda = \partial_t g, \qquad \partial_t\lambda(0) = \lambda(0) = 0,$$

where g is sufficiently smooth with $g(0) = g'(0) = 0$. This is formalized in

Lemma 3.3. *Let $g \in C^2(\mathbb{R}_+)$ be s.t. $g(0) = g'(0) = g^{(2)}(0) = 0$ and $g^{(3)} \in L^1_{loc}(\mathbb{R}_+)$. Let λ_ℓ, $\ell \in \mathbb{N}_*$, solve the system of ODEs:*

$$\frac{d^2}{dt^2}\lambda_\ell + \omega^2_\ell\lambda_\ell = \frac{d}{dt}g, \qquad \lambda_\ell(0) = \frac{d}{dt}\lambda_\ell(0) = 0. \tag{3.6}$$

Then

(1) the series $\sum_{\ell=1}^{\infty} a_\ell \frac{d\lambda_\ell}{dt}(t)$ converges uniformly on compact subsets of $[0, \infty)$.

(2) if, for all $t > 0$, $|g(t)| \le C(1 + t^m)$, with some C, $m \ge 0$, then

$$\mathbf{\Lambda}(\partial_t)g(t) = \mathbf{\Lambda}(0)g(t) + \sum_{\ell=1}^{\infty} a_\ell \frac{d\lambda_\ell}{dt}. \tag{3.7}$$

Before proving the above, let us state the following technical lemma.

Lemma 3.4. *The series* $S = \sum_{\ell=1}^{\infty} \frac{a_\ell}{\omega_\ell^2}$ *converges.*

Proof. By Theorem 3.1, provided $r \in (0, \omega_0)$, the series $S_r = \sum_{\ell=1}^{\infty} \frac{a_\ell r^2}{\omega_\ell^2 - r^2}$ converges. We conclude by noticing that $|S| < r^{-2} S_r$. □ □

Proof of Lemma 3.3. Let us first prove the statement about the convergence of $\sum_{\ell=1}^{\infty} a_\ell \frac{d\lambda_\ell}{dt}$. For this we will re-express λ_ℓ so that the general term of the series contains a term $\frac{a_\ell}{\omega_\ell^2}$. An explicit solution to (3.6) is given by

$$\lambda_\ell = \omega_\ell^{-1} \int_0^t \sin \omega_\ell (t-\tau) \frac{dg}{d\tau} d\tau, \qquad \text{hence} \quad \frac{d\lambda_\ell}{dt} = \int_0^t \cos \omega_\ell (t-\tau) \frac{dg}{d\tau} d\tau,$$

because $g'(0) = 0$. Integrating by parts twice, we obtain

$$\frac{d\lambda_\ell}{dt} = \omega_\ell^{-2} \frac{d^2 g}{dt^2} - \omega_\ell^{-2} \int_0^t \cos \omega_\ell (t-\tau) \frac{d^3 g(\tau)}{d\tau^3} d\tau, \tag{3.8}$$

where we again used $g'(0) = g''(0) = 0$. Hence,

$$\sum_{\ell=1}^{\infty} a_\ell \left| \frac{d\lambda_\ell}{dt} \right| \le \sum_{\ell=1}^{\infty} \frac{a_\ell}{\omega_\ell^2} \left(\left| \frac{d^2 g}{dt^2} \right| + \int_0^t |g^{(3)}(\tau)| d\tau \right),$$

which shows the uniform convergence of the series $\sum_{\ell=1}^{\infty} a_\ell \frac{d\lambda_\ell}{dt}(t)$.

To show 2., it suffices to prove that the expression in the right-hand side of (3.7) is the inverse Fourier-Laplace transform of $\mathbf{\Lambda}(\omega)\hat{g}(\omega)$. This follows by a direct computation, cf. (3.5) (the polynomial bound on g is used to ensure that $\hat{g}(\omega)$ is analytic in $\mathbb{C}^+$). □

3.1.2. *Approximating the reference DtN.* Based on the above, it is natural to approximate the reference DtN operator by truncating the series (3.7) to N terms:

$$\mathbf{\Lambda}^N(\partial_t) g = \mathbf{\Lambda}(0) g(t) + \sum_{\ell=1}^{N} a_\ell \frac{d\lambda_\ell}{dt}(t), \tag{3.9}$$

where λ_ℓ are defined in (3.6). In the Fourier-Laplace domain this amounts to replacing $\mathbf{\Lambda}(\omega)$ in (2.9) by the truncated series:

$$\mathbf{\Lambda}^N(\omega) = \mathbf{\Lambda}(0) - \sum_{\ell=1}^{N} \frac{a_\ell \omega^2}{\omega_\ell^2 - \omega^2}. \tag{3.10}$$

The respective error is controlled by the remainder of the series S from Lemma 3.4

$$r_N := \sum_{\ell=N+1}^{\infty} a_\ell \omega_\ell^{-2}, \tag{3.11}$$

and is quantified in the following lemma.

Lemma 3.5. *Let $g \in C^2(\mathbb{R}_+)$ be s.t. $g(0) = g'(0) = g^{(2)}(0) = 0$, $g^{(3)} \in L^1_{loc}(\mathbb{R}_+)$, and $|g(t)| \le C(1+t^m)$, with some $m, C \ge 0$. Then*

$$\left|\mathbf{\Lambda}(\partial_t)g(t) - \mathbf{\Lambda}^N(\partial_t)g(t)\right| \le 2r_N \int_0^t |g^{(3)}(\tau)|d\tau. \tag{3.12}$$

Proof. Comparing (3.7) and (3.9), we obtain,

$$\left|\mathbf{\Lambda}(\partial_t)g - \mathbf{\Lambda}^N(\partial_t)g\right| = \left|\sum_{\ell=N+1}^{\infty} a_\ell \frac{d}{dt}\lambda_\ell\right| \le \sum_{\ell=N+1}^{\infty} \frac{a_\ell}{\omega_\ell^2}\left(\left|g^{(2)}(t)\right| + \int_0^t |g^{(3)}|d\tau\right),$$

where the last inequality follows from (3.8). It remains to bound $\left|g^{(2)}\right|$ by $\int_0^t |g^{(3)}|d\tau$. □

3.2. **Coupled problem: formulation, stability and error analysis.**

3.2.1. *Formulation.* Let us consider (2.11) with $\mathcal{B}_m(\partial_t)$ replaced by the truncated DtN operator $\mathcal{B}^N_m(\partial_t)$, defined as, cf. (2.10),

$$\mathcal{B}^N_m(\partial_t) = \operatorname{diag}\left(\mathcal{B}^N_{m,0}(\partial_t), \dots, \mathcal{B}^N_{m,p^m-1}(\partial_t)\right),$$

where each $\mathcal{B}^N_{m,j}(\partial_t)$ is expressed via the truncated reference DtN, cf. (2.9):

$$\mathcal{B}^N_{m,j}(\partial_t) = \mu_{m,j}\alpha^{-1}_{m,j}\sum_{k=0}^{p-1}\frac{\mu_k}{\alpha_k}\mathbf{\Lambda}^N(\alpha_k\alpha_{m,j}\partial_t). \tag{3.13}$$

These are the operators with the following symbols:

$$\mathcal{B}^N_{m,j}(\partial_t) = \mu_{m,j}\alpha^{-1}_{m,j}\left(\left\langle\frac{\boldsymbol{\mu}}{\boldsymbol{\alpha}}\right\rangle\mathbf{\Lambda}(0) - \sum_{k=0}^{p-1}\frac{\mu_k}{\alpha_k}\sum_{n=1}^{N}\frac{a_n\omega^2}{(\alpha^{-1}_{m,j}\alpha_k^{-1}\omega_n)^2-\omega^2}\right). \tag{3.14}$$

Replacing $\mathcal{B}_m(\partial_t)$ in (2.11) by $\mathcal{B}^N_m(\partial_t)$ leads to the following problem: find

$$u_N \in C^2([0,T];\mathrm{L}^2_\mu(\mathcal{T}^m)) \cap C^1([0,T];\mathbf{V}_\mu(\mathcal{T}^m)),\ \text{s.t. } u_N(.,0) = \partial_t u_N(.,0) = 0,$$

that satisfies for all $v \in V_\mu(\mathcal{T}^m)$

$$(\partial_t^2 u_N, v)_{\mathcal{T}^m} + (\partial_s u_N, \partial_s v)_{\mathcal{T}^m} + \int_{\Gamma_m}\mathcal{B}^N_m(\partial_t)\boldsymbol{u}_N\,\boldsymbol{v} = (f,v)_{\mathcal{T}^m},\ \text{where} \tag{3.15a}$$

$$\mathcal{B}^N_m(\partial_t)\boldsymbol{\gamma}_m u_N = \mathbf{W}_m\mathbf{D}_m\left(\left\langle\frac{\boldsymbol{\mu}}{\boldsymbol{\alpha}}\right\rangle\mathbf{\Lambda}(0)\boldsymbol{\gamma}_m u_N + \sum_{k=0}^{p-1}\frac{\mu_k}{\alpha_k}\sum_{\ell=1}^{N}a_\ell\partial_t\boldsymbol{\lambda}^N_{\ell,k}\right), \tag{3.15b}$$

$$\mathbf{D}_m = \operatorname{diag}\left(\alpha^{-1}_{m,0},\dots,\alpha^{-1}_{m,p^m-1}\right),\quad \mathbf{W}_m = \operatorname{diag}\left(\mu_{m,0},\dots,\mu_{m,p^m-1}\right), \tag{3.15c}$$

and the vector-valued functions $\boldsymbol{\lambda}^N_{\ell,k} : \mathbb{R}_+ \to \mathbb{R}^{p^m}$ satisfy

$$\partial_t^2\boldsymbol{\lambda}^N_{\ell,k} + \alpha_k^{-2}\omega_\ell^2\mathbf{D}^2_m\boldsymbol{\lambda}^N_{\ell,k} = \partial_t\boldsymbol{\gamma}_m u_N, \qquad \boldsymbol{\lambda}^N_{\ell,k}\big|_{t=0} = \partial_t\boldsymbol{\lambda}^N_{\ell,k}\big|_{t=0} = 0. \tag{3.15d}$$

3.2.2. *Stability of the formulation (3.15).* Stability of the formulation (3.15) is guaranteed by non-negativity of $\mathbf{\Lambda}(0)$ and a_n, $n \in \mathbb{N}$, in (3.14), see Theorem 3.1.

Theorem 3.6 (Stability)**.** *Let $f \in L^1(0,\, T; \mathrm{L}^2_\mu(\mathcal{T}^m))$. Then the solution of (3.15) satisfies the following bound:*

$$\sqrt{\mathcal{E}_N(T)} \leq C \int_0^T \|f(t)\|_{\mathrm{L}^2_\mu(\mathcal{T}^m)} dt,$$

where

$$\mathcal{E}_N = \frac{1}{2}\left(\|\partial_t u_N\|^2_{\mathcal{T}^m} + \|\partial_s u_N\|^2_{\mathcal{T}^m} + \left\langle \frac{\boldsymbol{\mu}}{\boldsymbol{\alpha}} \right\rangle \mathbf{\Lambda}(0) \int_{\Gamma_m} \frac{\boldsymbol{\mu}}{\boldsymbol{\alpha}} |\boldsymbol{u}|^2 \right) + \mathcal{E}_{N,\lambda},$$

$$\mathcal{E}_{N,\lambda} = \frac{1}{2} \sum_{k=0}^{p-1} \sum_{\ell=1}^{N} a_\ell \frac{\mu_k}{\alpha_k} \left(\int_{\Gamma_m} \frac{\boldsymbol{\mu}}{\boldsymbol{\alpha}} \left|\partial_t \boldsymbol{\lambda}^N_{\ell,k}\right|^2 + \alpha_k^{-2} \omega_\ell^2 \int_{\Gamma_m} \frac{\boldsymbol{\mu}}{\boldsymbol{\alpha}^3} |\boldsymbol{\lambda}^N_{\ell,k}|^2 \right). \tag{3.16}$$

Proof. The proof is classical. It suffices to test (3.15a) with $v = \partial_t u$, and notice that, thanks to (3.15d), with $\langle ., . \rangle$ denoting the Eucledian scalar product in $\mathbb{R}^{p^m}$,

$$\langle \mathbf{W}_m \mathbf{D}_m \partial_t \boldsymbol{\lambda}^N_{\ell,k}, \partial_t \boldsymbol{\gamma}_m u \rangle = \frac{1}{2} \frac{d}{dt} \left(\int_{\Gamma_m} \frac{\boldsymbol{\mu}}{\boldsymbol{\alpha}} \left|\partial_t \boldsymbol{\lambda}^N_{\ell,k}\right|^2 + \alpha_k^{-2} \omega_\ell^2 \int_{\Gamma_m} \frac{\boldsymbol{\mu}}{\boldsymbol{\alpha}^3} |\boldsymbol{\lambda}^N_{\ell,k}|^2 \right).$$

This results in the energy identity

$$\frac{d}{dt} \mathcal{E}_N = (f, \partial_t u_N)_{\mathcal{T}^m}.$$

The rest follows by a straightforward application of the Gronwall's lemma. □

3.3. **Error analysis for (3.15).** Here we study the error of approximating (2.11) by (3.15) as a function of the number of the terms in the truncated series N, as $N \to \infty$. Additionally, we will be interested in the behaviour of this error as a function of m (the level at which the tree is truncated). Nonetheless, we consider that this is of less importance, the reason being that the complexity of resolution of (3.15) increases exponentially with m, since at the m-th level there are p^m branches of the tree. At the same time, the complexity of resolution of (3.15) is linear in N.

The principal result of this section is summarized below.

Theorem 3.7. *Given $f \in W^{4,1}(0, T; \mathrm{L}^2_\mu(\mathcal{T}))$, s.t. $f(0) = \ldots = f^{(3)}(0) = 0$, let u solve either (D) or (N), and u_N solve (3.15) with Dirichlet (or Neumann) absorbing boundary conditions. Let $\varepsilon_N = u_N - u|_{\mathcal{T}^m}$. With r_N defined in (3.11),*

(1) when $\left\langle \boldsymbol{\mu}\boldsymbol{\alpha} \right\rangle < 1$,

$$\|\partial_t \varepsilon_N(T)\|_{\mathrm{L}^2_\mu(\mathcal{T}^m)} + \|\partial_s \varepsilon_N(T)\|_{\mathrm{L}^2_\mu(\mathcal{T}^m)} \leq C r_N m^2 \eta^m T \|\partial_t^4 \partial_s u\|_{L^1(0,T;\mathrm{L}^2_\mu(\mathcal{T}))},$$

where $\eta = \max(\left\langle \boldsymbol{\mu}\boldsymbol{\alpha} \right\rangle, |\boldsymbol{\alpha}|^2_\infty)$.

(2) when $\left\langle \boldsymbol{\mu}\boldsymbol{\alpha} \right\rangle \geq 1$,

$$\|\partial_t \varepsilon_N(T)\|_{\mathrm{L}^2_\mu(\mathcal{T}^m)} + \|\partial_s \varepsilon_N(T)\|_{\mathrm{L}^2_\mu(\mathcal{T}^m)} \leq C r_N |\boldsymbol{\alpha}|^{2m}_\infty T \|\partial_t^4 \partial_s u\|_{L^1(0,T;\mathrm{L}^2_\mu(\mathcal{T}\setminus\mathcal{T}^m))}.$$

The constant $C > 0$ depends on $\boldsymbol{\alpha}, \boldsymbol{\mu}$ only.

Let us comment on the above result:

- obviously, for fixed T, m, as $N \to \infty$, $\|\varepsilon_N\|_{\mathrm{L}^2_\mu(\mathcal{T}^m)} \to 0$ (see Lemma 3.4),
- when N, T are fixed, as $m \to \infty$, $\|\varepsilon_N\|_{\mathrm{L}^2_\mu(\mathcal{T}^m)} \to 0$.

Proof of Theorem 3.7. First of all, let us remark that the regularity condition on the source term f ensures the required regularity of the solution u, see [9].

Step 1. Re-expressing ε_N. The error ε_N solves the following problem: find $\varepsilon_N \in \mathbf{V}_\mu(\mathcal{T}^m)$, s.t. $\varepsilon_N|_{t=0} = \partial_t \varepsilon_N|_{t=0} = 0$, and for all $v \in \mathbf{V}_\mu(\mathcal{T}^m)$,

$$\left(\partial_t^2 \varepsilon_N, v\right)_{\mathcal{T}^m} + (\partial_s \varepsilon_N, \partial_s v)_{\mathcal{T}^m} + \int\limits_{\Gamma_m} \left(\mathcal{B}_m^N(\partial_t)\boldsymbol{u}_N - \mathcal{B}_m(\partial_t)\boldsymbol{u}\right)\boldsymbol{v} = 0.$$

Defining

$$\boldsymbol{\zeta}_m^N = \left(\mathcal{B}_m(\partial_t) - \mathcal{B}_m^N(\partial_t)\right)\boldsymbol{\gamma}_m u(t), \tag{3.17}$$

we rewrite the above in the form (3.15a):

$$\left(\partial_t^2 \varepsilon_N, v\right)_{\mathcal{T}^m} + (\partial_s \varepsilon_N, \partial_s v)_{\mathcal{T}^m} + \int\limits_{\Gamma_m} \mathcal{B}_m^N(\partial_t)\boldsymbol{\varepsilon_N}\boldsymbol{v} = \int\limits_{\Gamma_m} \boldsymbol{\zeta}_m^N \boldsymbol{v}.$$

Testing the above with $v = \partial_t \varepsilon_N$, and introducing the error energy, see Theorem 3.6,

$$\mathcal{E}_{N,\varepsilon} = \frac{1}{2}\left(\|\partial_t \varepsilon_N\|^2_{\mathrm{L}^2_\mu(\mathcal{T}^m)} + \|\partial_s \varepsilon_N\|^2_{\mathrm{L}^2_\mu(\mathcal{T}^m)} + \left\langle \frac{\boldsymbol{\mu}}{\boldsymbol{\alpha}} \right\rangle \boldsymbol{\Lambda}(0) \int\limits_{\Gamma_m} \frac{\boldsymbol{\mu}}{\boldsymbol{\alpha}} |\boldsymbol{\varepsilon}_N|^2\right) + \mathcal{E}_{N,\lambda_\varepsilon}, \tag{3.18}$$

with $\mathcal{E}_{N,\lambda_\varepsilon}$ defined like in (3.16), we obtain the following expression:

$$\frac{d}{dt}\mathcal{E}_{N,\varepsilon} = \int\limits_{\Gamma_m} \boldsymbol{\zeta}_m^N(t)\partial_t \boldsymbol{\varepsilon}_N(t). \tag{3.19}$$

Integrating the above from 0 to T results in

$$\mathcal{E}_{N,\varepsilon}(T) = \int\limits_{\Gamma_m} \boldsymbol{\zeta}_m^N(T)\boldsymbol{\varepsilon}_N(T) - \int\limits_0^T \int\limits_{\Gamma_m} \partial_t \boldsymbol{\zeta}_m^N(t)\boldsymbol{\varepsilon}_N(t)dt. \tag{3.20}$$

Step 2. Bounding the right-hand side of (3.20). The following bound is a direct corollary of representation (3.13):

$$\left|\int\limits_{\Gamma_m} \boldsymbol{\zeta}_N \boldsymbol{v}\right| \leq \sum_{k=0}^{p-1} \frac{\mu_k}{\alpha_k} \int\limits_{\Gamma_m} \boldsymbol{\mu}\boldsymbol{\alpha}^{-1} \left|\boldsymbol{\Lambda}^N(\alpha_k \boldsymbol{\alpha}\partial_t)\boldsymbol{u} - \boldsymbol{\Lambda}(\alpha_k \boldsymbol{\alpha}\partial_t)\boldsymbol{u}\right| |\boldsymbol{v}|.$$

Because

$$\boldsymbol{\Lambda}(\alpha_k \alpha_{m,j}\omega) = \boldsymbol{\Lambda}(0) - \sum_{\ell=1}^{\infty} \frac{a_\ell \omega^2}{(\alpha_k^{-1}\alpha_{m,j}^{-1}\omega_\ell)^2 - \omega^2},$$

the above in turn can be bounded by, cf. (3.12),

$$\left|\int_{\Gamma_m} \boldsymbol{\zeta}_N \boldsymbol{v}\right| \le 2r_N \sum_{k=0}^{p-1} \frac{\mu_k}{\alpha_k} \int_{\Gamma_m} \boldsymbol{\mu}\boldsymbol{\alpha}^{-1}\alpha_k^2\boldsymbol{\alpha}^2 \left(\int_0^t |\partial_\tau^3 \boldsymbol{u}(\tau)|d\tau\right) |\boldsymbol{v}|$$

$$= 2r_N\langle\boldsymbol{\mu}\boldsymbol{\alpha}\rangle \int_{\Gamma_m} \boldsymbol{\mu}\boldsymbol{\alpha}|\boldsymbol{v}| \int_0^t |\partial_\tau^3 \boldsymbol{u}(\tau)|d\tau. \tag{3.21}$$

With the bound (3.21), (3.20) can be rewritten as follows:

$$\mathcal{E}_{N,\varepsilon}(T) \le 2r_N\langle\boldsymbol{\mu}\boldsymbol{\alpha}\rangle \left(\int_0^T \int_{\Gamma_m} \boldsymbol{\mu}\boldsymbol{\alpha} \left(|\partial_t^3 \boldsymbol{u}(t)| + \int_0^t |\partial_\tau^4 \boldsymbol{u}(\tau)|d\tau\right) |\boldsymbol{\varepsilon}_N(t)|dt\right)$$

$$\le 4r_N\langle\boldsymbol{\mu}\boldsymbol{\alpha}\rangle \int_0^T \int_0^t \int_{\Gamma_m} \boldsymbol{\mu}\boldsymbol{\alpha}|\partial_\tau^4 \boldsymbol{u}(\tau)||\boldsymbol{\varepsilon}_N(t)|d\tau\, dt, \tag{3.22}$$

where we used the bound $|\partial_t^3 \boldsymbol{u}(t)| \le |\partial_t^4 \boldsymbol{u}(t)|_{L^1(0,t)}$.

Step 3. Bounding ε_N based on (3.22). Naturally, we would like to apply a Gronwall inequality to the above. This is where the different treatment of the cases $\langle\boldsymbol{\mu}\boldsymbol{\alpha}\rangle <$ and $\langle\boldsymbol{\mu}\boldsymbol{\alpha}\rangle \ge 1$ begins. When $\langle\boldsymbol{\mu}\boldsymbol{\alpha}\rangle < 1$, for the Neumann problem $\boldsymbol{\Lambda}(0) = 0$, see Proposition 3.2, and thus the boundary term in (3.18) does not control $\boldsymbol{\gamma}_m\varepsilon_N(T)$. Hence, in this case we will use a certain trace continuity result. The obtained bound on the error will be still valid when $\langle\boldsymbol{\mu}\boldsymbol{\alpha}\rangle \ge 1$, but it is highly non-optimal (in fact, when $\langle\boldsymbol{\mu}\boldsymbol{\alpha}\rangle \ge 1$, this bound does not prevent the error from growing exponentially as m increases). This is why we will deal with the case $\langle\boldsymbol{\mu}\boldsymbol{\alpha}\rangle \ge 1$ separately.

Error bound when $\langle\boldsymbol{\mu}\boldsymbol{\alpha}\rangle < 1$. We start with an auxiliary lemma.

Lemma 3.8 (Trace continuity)**.** *Let $v \in \boldsymbol{V}_\mu(\mathcal{T}^m)$. Then, for all $m \ge 1$,*

$$\int_{\Gamma_m} \boldsymbol{\mu}\boldsymbol{\alpha}|\boldsymbol{v}|^2 \le C_{\boldsymbol{\alpha},\boldsymbol{\mu}} m^2\eta^m \|\partial_s v\|^2_{\mathrm{L}^2_\mu(\mathcal{T}^m)}, \quad \eta = \max(\langle\boldsymbol{\mu}\boldsymbol{\alpha}\rangle, |\boldsymbol{\alpha}|^2_\infty), \tag{3.23}$$

where $C_{\boldsymbol{\alpha},\boldsymbol{\mu}}$ is independent of m.

The proof of this result can be found in Appendix A. It remains to use the above to bound (3.22). Application of the Cauchy-Schwartz inequality yields

$$\mathcal{E}_{N,\varepsilon}(T) \le 4r_N\langle\boldsymbol{\mu}\boldsymbol{\alpha}\rangle \int_0^T \int_0^t \left(\int_{\Gamma_m} \boldsymbol{\mu}\boldsymbol{\alpha}|\partial_\tau^4 \boldsymbol{u}(\tau)|^2\right)^{\frac{1}{2}} \left(\int_{\Gamma_m} \boldsymbol{\mu}\boldsymbol{\alpha}|\varepsilon_N(t)|^2\right)^{\frac{1}{2}} d\tau\, dt$$

$$\overset{(3.23)}{\le} Cr_N m^2\eta^m \int_0^T \left(\int_0^t \|\partial_s\partial_\tau^4 u(\tau)\|_{\mathrm{L}^2_\mu(\mathcal{T}^m)}d\tau\right) \|\partial_s\varepsilon_N(t)\|_{\mathrm{L}^2_\mu(\mathcal{T}^m)}\, dt,$$

where the constant C does not depend on T, m or N. With Gronwall's inequality,

$$\sqrt{\mathcal{E}_{N,\varepsilon}(T)} \le Cr_N m^2\eta^m T\|\partial_s\partial_\tau^4 u\|_{L^1(0,T;\mathrm{L}^2_\mu(\mathcal{T}^m))}.$$

As $m \to \infty$, $\mathcal{E}_{N,\varepsilon}(T) \to 0$, because $\eta = \max(\langle\boldsymbol{\mu}\boldsymbol{\alpha}\rangle, |\boldsymbol{\alpha}|^2_\infty) < 1$. When $\langle\boldsymbol{\mu}\boldsymbol{\alpha}\rangle \ge 1$, this is no longer the case, and thus a different approach is needed.

Error bound when $\langle \boldsymbol{\mu\alpha} \rangle \geq 1$. Recall that in this case we can control $\boldsymbol{\gamma}_m \varepsilon_N$ in (3.22) by $\mathcal{E}_{N,\varepsilon}$, because $\boldsymbol{\Lambda}(0) \neq 0$, see Theorem 3.2, cf. the definition of $\mathcal{E}_{N,\varepsilon}$ (3.18).

Like before, we start by bounding (3.22). With the Cauchy-Schwartz inequality,

$$\mathcal{E}_{N,\varepsilon}(T) \leq 4 r_N \langle \boldsymbol{\mu\alpha} \rangle \int_0^T \int_0^t \left(\int_{\Gamma_m} \boldsymbol{\mu\alpha}^3 |\partial_\tau^4 \boldsymbol{u}|^2 \right)^{\frac{1}{2}} d\tau \left(\int_{\Gamma_m} \boldsymbol{\mu\alpha}^{-1} |\boldsymbol{\varepsilon}_N(t)|^2 \right)^{\frac{1}{2}} dt. \tag{3.24}$$

Remarking that, cf. (2.6),

$$\int_{\Gamma_m} \boldsymbol{\mu\alpha}^3 |\partial_\tau^4 \boldsymbol{u}|^2 \leq \max_j \alpha_{m,j}^4 \int_{\Gamma_m} \boldsymbol{\mu\alpha}^{-1} |\partial_\tau^4 \boldsymbol{u}|^2 \leq |\boldsymbol{\alpha}|^{-4m} \int_{\Gamma_m} \boldsymbol{\mu\alpha}^{-1} |\partial_\tau^4 \boldsymbol{u}|^2,$$

and controlling $\int_{\Gamma_m} \boldsymbol{\mu\alpha}^{-1} |\boldsymbol{\varepsilon}_N|^2$ by $\mathcal{E}_{N,\varepsilon}(t)$, we deduce from (3.24)

$$\mathcal{E}_{N,\varepsilon}(T) \leq C r_N \langle \boldsymbol{\mu\alpha} \rangle |\boldsymbol{\alpha}|_\infty^{2m} \int_0^T \int_0^t \left(\int_{\Gamma_m} \boldsymbol{\mu\alpha}^{-1} |\partial_\tau^4 \boldsymbol{u}|^2 \right)^{\frac{1}{2}} d\tau \sqrt{\mathcal{E}_{N,\varepsilon}(t)} dt.$$

The constant $C > 0$ does not depend on T, N, m. Gronwall's inequality yields

$$\sqrt{\mathcal{E}_{N,\varepsilon}(T)} \leq C r_N |\boldsymbol{\alpha}|_\infty^{2m} T \int_0^T \left(\int_{\Gamma_m} \boldsymbol{\mu\alpha}^{-1} |\partial_t^4 \boldsymbol{u}|^2 \right)^{\frac{1}{2}} dt.$$

To bound the rhs in the above, we use the following inequality from [10, Theorem 3.18, the end of the proof]

$$\left(\int_{\Gamma_m} \boldsymbol{\mu\alpha}^{-1} |\partial_t^4 \boldsymbol{u}|^2 \right)^{\frac{1}{2}} \leq C \|\partial_t^4 \partial_s u\|_{\mathrm{L}^2_\mu(\mathcal{T} \setminus \mathcal{T}^m)}.$$

□

The error estimates provided by Theorem 3.7 are explicit in m, however, depend on N non-trivially, via the remainder of the series r_N, defined in (3.11). It is natural to ask how many terms in the truncated expansion should be chosen to ensure that $r_N < \varepsilon$, for a given accuracy ε. This is the subject of the following section.

4. Quantitative estimates of the error as $N \to \infty$

From (3.11) and Theorem 3.1 it follows that the behaviour of r_N as $N \to +\infty$ is quantified by

(i) an asymptotic behaviour of the eigenvalues ω_n^2 of the weighted Laplacian;
(ii) an asymptotic behaviour of the coefficients $a_n = \omega_n^{-2} \left(\partial_s \varphi_n(M^*) \right)^2$.

A natural approach to estimate r_N would be to use a uniform bound on a_n, i.e. $a_n < C$, for some $C > 0$ (which is easy to prove), and an asymptotic estimate on $\omega_n^2 \geq c(n)$. However, it appears that this bound can be very pessimistic: depending on the geometry of the fractal tree, the respective majorating series

$$r_N \leq C \sum_{n=N+1}^{\infty} c(n)^{-1}$$

may not converge. Nonetheless, based on the numerical experiments, we conjecture that the uniform bound for a_n is optimal, in a sense that there exists $C_* > 0$, s.t. for all n_* there exists $n > n_*$ s.t. $a_n > C_*$. The optimality seems to hold true (for most of the geometries) for $c(n)$ as well. This is why this strategy is not well-suited for estimating r_N.

Another subtlety in bounding r_N as a function of N lies in the fact that in some cases the poles of $\mathbf{\Lambda}_{\mathfrak{a}}(\omega)$ (which are of importance for the approximation (3.15b)) constitute a **proper subset** of the eigenvalues of operators $\mathcal{A}_{\mathfrak{a}}$, because $\varphi_n(M^*)$ and $\partial_s\varphi_n(M^*)$ may vanish simultaneously. This is very different from the situation of a non-weighted Laplacian with mixed/Dirichlet boundary conditions on Lipschitz domains. In particular, this implies that the asymptotic behaviour of the eigenvalues ω_n^2 of the weighted Laplacian may differ from the asymptotics of the poles of $\mathbf{\Lambda}(\omega)$.

For these reasons, in order to provide an estimate for r_N (and, accordingly, an estimate for the asymptotic complexity of the method presented in this article), we adapt a somewhat different point of view.

4.1. **Introduction: an alternative strategy for the error control. Summary of the main results.**

4.1.1. *Controlling the remainder of the series S from Lemma 3.4.* As discussed before, instead of examining r_N, we will work with an alternative quantity

$$R_\omega = \sum_{n:\,\omega_n \geq \omega} \frac{a_n}{\omega_n^2}, \qquad \omega > 0. \tag{4.1}$$

Theorem 4.1. *There exists $C > 0$, that depends on $\boldsymbol{\alpha}, \boldsymbol{\mu}$ only, s.t. $R_\omega \leq C\,\omega^{-1}$.*

The proof of Theorem 4.1 is based on a trivial adaptation of the estimates on a_n, which follow from the results by Barnett and Hassell [3] re-interpreted in 1D. Instead of bounding each a_n separately, we will rather work with the 'package'

$$\sum_{j:\,|\omega_j-\omega|<\eta} (\partial_s\varphi_j(0))^2\omega_j^{-2} = \sum_{j:\,|\omega_j-\omega|<\eta} a_j. \tag{4.2}$$

In [3] the authors show that the above quantity is uniformly bounded in ω. This improves the trivial bound

$$\sum_{j:\,|\omega_j-\omega|<\eta} a_j \leq \#\{\omega_j :\, |\omega_j-\omega|<\eta\} \max_{k\geq 1} a_k,$$

which depends on the number of eigenfunctions on the interval $(\omega-\eta, \omega+\eta)$. In particular, as can be seen from the results of Theorem 4.8, in the case of fractals this quantity may grow arbitrarily fast.

Lemma 4.2. *For any $\eta, \omega > 0$, $\displaystyle\sum_{j:\,|\omega_j-\omega|<\eta} (\partial_s\varphi_j(0))^2\omega_j^{-2} \equiv \sum_{j:\,|\omega_j-\omega|<\eta} a_j \leq C_\eta$.*

Proof. See Appendix B. □

Proof of Theorem 4.1. Because R_ω is non-increasing, it suffices to prove Theorem 4.1 for $\omega \in \mathbb{N}_*$. Taking $\omega = m \in \mathbb{N}_*$, we rewrite (4.1) in the following form

$$R_m = \sum_{n:\,\omega_n \geq m} \frac{a_n}{\omega_n^2} = \sum_{n=m}^{\infty} \sum_{n\leq\omega_j<n+1} \frac{a_j}{\omega_j^2},$$

where, in order to apply Lemma 4.2, we split the interval $[m,\infty)$ into subintervals $[k,k+1)$, $k\geq m$ and sum over eigenvalues belonging to these intervals. Obviously,

$$R_m \leq \sum_{n=m}^{\infty} \sum_{n-1\leq\omega_j<n+1} \frac{a_j}{\omega_j^2} \leq \sum_{n=m}^{\infty} \frac{1}{n^2} \sum_{|\omega_j-n|\leq 1} a_j \leq C\sum_{n=m}^{\infty}\frac{1}{n^2},$$

where the last bound follows from Lemma 4.2 applied with $\eta=1$. The above remainder is $O(m^{-1})$. □

The bound of Theorem 4.1 is optimal, according to the following theorem.

Theorem 4.3. *There exists $c>0$, that depends on $\boldsymbol{\alpha},\boldsymbol{\mu}$ only, s.t. for all ω sufficiently large, $R_\omega \geq c\,\omega^{-1}$.*

The proof of this result almost mimics the proof of Theorem 4.1, and relies on the following counterpart of Lemma 4.2. The proof of this result is based on very different ideas from the ones used in the proof of Lemma 4.2.

Lemma 4.4. *There exists $\eta_*>0$, s.t. for all $\eta>\eta_*$, there exists $C_\eta>0$, s.t. for all $\omega>1$,*

$$\sum_{j:\,|\omega_j-\omega|<\eta} (\partial_s\varphi_j(0))^2\omega_j^{-2} \equiv \sum_{j:\,|\omega_j-\omega|<\eta} a_j \geq C_\eta. \tag{4.3}$$

Proof. See Appendix C. □

Let us remark that because in the above result we are interested in the lower bound on the quantities (4.2), the above lower bound does not necessarily hold for $\eta_*=0$. This becomes clear when one examines the case $p=1$ and $\mu_0=1$, when the tree $\mathcal{T}$ reduces to an interval and ω_j to the spectrum of the Dirichlet/mixed Laplacian on an interval. Indeed, in this case, there exists $c>0$, s.t. for any $j\neq k$, $|\omega_j-\omega_k|>c$, and hence, for sufficiently small η, the sum in (4.2) may contain no terms, however large ω is chosen.

Proof of Theorem 4.3. Let us fix $\eta:=\ell\geq 1$ integer and large enough, so that the conditions of Lemma 4.4 hold true. Like before, let us consider R_ω with $\omega=m$, i.e. $R_m=\sum_{n:\,\omega_n>m}\frac{a_n}{\omega_n^2}$. We assume that $\omega=m>\ell$. Because we would like to apply the result of Lemma 4.4, we use the same trick like in the proof of Theorem 4.1, namely, we split the interval $[m,\infty)$ into smaller intervals of width 2ℓ that do not intersect. I.e.

$$[m,\infty)=[(m+\ell)-\ell,(m+\ell)+\ell)\cup[(m+3\ell)-\ell,\,(m+3\ell)+\ell)\cup\dots$$

With a shortened notation, $I_k:=[(m+k\ell)-\ell,\,(m+k\ell)+\ell)$, we rewrite

$$R_m=\sum_{k=1}^{\infty}\sum_{\omega_n\in I_{2k-1}}\frac{a_n}{\omega_n^2}\geq\sum_{k=1}^{\infty}\frac{1}{\left((m+k\ell)-\ell\right)^2}\sum_{\omega_n\in I_{2k-1}}a_n.$$

By Lemma 4.4, applied with $\omega=m+k\ell$ and $\eta=\ell$,

$$\sum_{\omega_n\in I_{2k-1}}a_n\geq C_\ell>0.$$

Therefore, for any $m > \ell$,

$$R_m \geq C_\ell \sum_{k=1}^{\infty} \frac{1}{\left(m + (k-1)\ell\right)^2}$$

Taking $m = N\ell$, where $N \in \mathbb{N}$, we in particular obtain

$$R_m \geq C_\ell\, \ell^{-2} \sum_{k=1}^{\infty} \frac{1}{\left(N + (k-1)\right)^2} \geq \frac{\tilde{C}_\ell}{N\ell^2} = \frac{\tilde{C}_\ell}{m\ell}.$$

As R_ω is non-increasing, we deduce that $R_\omega \geq c\,\omega^{-1}$ for all ω sufficiently large. □

The above results show that to ensure that $c\,\varepsilon < r_N < C\,\varepsilon$ it is necessary to take $N = N_{\mathfrak{a},\varepsilon}$, where $N_{\mathfrak{a},\varepsilon}$ is the number of **positive poles** of $\mathbf{\Lambda}_{\mathfrak{a}}(\omega)$ lying inside the interval $(0, \varepsilon^{-1})$, i.e.

$$\begin{aligned} &N_{\mathfrak{a},\varepsilon} := \#\{n : \widetilde{\omega}_{\mathfrak{a},n} < \varepsilon^{-1}, \quad \widetilde{\omega}_{\mathfrak{a},n} \in \mathcal{P}_{\mathfrak{a}}\}, \text{ where} \\ &\mathcal{P}_{\mathfrak{a}} = \{0 < \widetilde{\omega}_{\mathfrak{a},1} < \widetilde{\omega}_{\mathfrak{a},2} < \ldots, \quad \widetilde{\omega}_{\mathfrak{a},j} \text{ is a positive pole of } \mathbf{\Lambda}_{\mathfrak{a}}\}. \end{aligned} \tag{4.4}$$

4.1.2. *Choice of the number of poles for the error control: main results.* To formulate the principal result of this section, let us introduce $d_s > 0$ (this number is also called the Minkowski dimension of $\mathcal{T}$, cf. [16]), s.t.

$$\sum_{i=0}^{p-1} \alpha_i^{d_s} = 1. \tag{4.5}$$

The existence and uniqueness of $d_s > 0$ follows by remarking that the function $x \to \sum_{i=0}^{p-1} \alpha_i^x$, $x \geq 0$, is strictly monotonically decaying from p to 0. Let additionally

$$\langle \boldsymbol{\alpha} \rangle := \sum_{i=0}^{p-1} \alpha_i . f \tag{4.6}$$

Theorem 4.5. *The following estimate holds for $N_{\mathfrak{a},\varepsilon}$, $\mathfrak{a} \in \{\mathfrak{d}, \mathfrak{n}\}$, defined in (4.4), with some $c_{\mathfrak{a}}$, $C_{\mathfrak{a}} > 0$ depending only on $\boldsymbol{\mu}$, $\boldsymbol{\alpha}$:*

- *if $\langle \boldsymbol{\alpha} \rangle < 1$ ($d_s < 1$), $c_{\mathfrak{a}}\, \varepsilon^{-1} \leq N_{\mathfrak{a},\varepsilon} \leq C_{\mathfrak{a}}\, \varepsilon^{-1}$.*
- *if $\langle \boldsymbol{\alpha} \rangle = 1$ ($d_s = 1$), $c_{\mathfrak{a}}\, \varepsilon^{-1} \leq N_{\mathfrak{a},\varepsilon} \leq C_{\mathfrak{a}}\, \varepsilon^{-1} \log \varepsilon^{-1}$.*
- *if $\langle \boldsymbol{\alpha} \rangle > 1$ ($d_s > 1$), $c_{\mathfrak{a}}\, \varepsilon^{-1} \leq N_{\mathfrak{a},\varepsilon} \leq C_{\mathfrak{a}}\, \varepsilon^{-d_s}$.*

Remark 4.6. Our numerical experiments suggest that in the absence of symmetries (i.e. when $\alpha_i \neq \alpha_j$ for $i \neq j$), the above upper bound is sharp (i.e., in particular, in the case $\langle \boldsymbol{\alpha} \rangle > 1$ $N_{\mathfrak{a},\varepsilon} \geq c_{\mathfrak{a}} \varepsilon^{-d_s}$ for some $c_{\mathfrak{a}} > 0$); however, we have no theoretical justification for this fact. Concerning symmetries, please see Section 4.2.4.

Using Theorems 4.1 and 4.3, the above result can be translated into the dependence of r_N on N.

Corollary 4.7 (Convergence rates)**.** For all $N \geq 1$, r_N defined in (3.11) satisfies the following estimate with c, C depending only on $\boldsymbol{\mu}$, $\boldsymbol{\alpha}$:

- if $\langle \boldsymbol{\alpha} \rangle < 1$ ($d_s < 1$), $cN^{-1} \leq r_N \leq CN^{-1}$.
- if $\langle \boldsymbol{\alpha} \rangle = 1$ ($d_s = 1$), $cN^{-1} \leq r_N \leq CN^{-1} \log N$.
- if $\langle \boldsymbol{\alpha} \rangle > 1$ ($d_s > 1$), $cN^{-1} \leq r_N \leq CN^{-\frac{1}{d_s}}$.

We will proceed as follows:

- in Section 4.2, we obtain an upper bound on $N_{\mathfrak{a},\varepsilon}$, by estimating the asymptotics for the counting function of the Dirichlet/Neumann eigenvalues:

$$\rho_{\mathfrak{a}}(\lambda) = \#\{\ell : \omega^2_{\mathfrak{a},\ell} < \lambda\}, \tag{4.7}$$

  where the eigenvalues are counted with their multiplicities.
- in Section 4.3 we prove a lower bound on $N_{\mathfrak{a},\varepsilon}$, valid in any case.
- in Section 4.4 we summarize the results in the proof of Theorem 4.5.

4.2. **An upper bound for $N_{\mathfrak{a},\varepsilon}$: asymptotics for counting functions.** Asymptotics for counting functions of the discrete and continuous Laplacian on various types of fractals were obtained in e.g. [14, 16, 2], see as well [12] and references therein. Our geometric setting bears some similarities to the one from the work by Levitin, Vassiliev [16], however, we do not use the same geometrical and boundary conditions assumptions. We will use as well some of the ideas from the seminal article by Kigami and Lapidus [14], whether the authors study an asymptotic distribution of eigenvalues for the discrete Laplacian on the post-critically finite self-similar fractals (the geometry considered in the present paper does not belong to this class).

The main result of this section is formulated in the following

Theorem 4.8. *The counting functions $\rho_{\mathfrak{a}}$, $\mathfrak{a} \in \{\mathfrak{d}, \mathfrak{n}\}$, satisfy for $\lambda \to +\infty$*

(1) if $\langle \boldsymbol{\alpha} \rangle < 1$ ($d_s < 1$), then $\rho_{\mathfrak{a}}(\lambda) = \pi^{-1} \left(1 - \langle \boldsymbol{\alpha} \rangle\right)^{-1} \lambda^{\frac{1}{2}} + O(\lambda^{\frac{d_s}{2}})$.

(2) if $\langle \boldsymbol{\alpha} \rangle = 1$ ($d_s = 1$), then $\rho_{\mathfrak{a}}(\lambda) = \pi^{-1} C_{\boldsymbol{\alpha}} \lambda^{\frac{1}{2}} \log \lambda^{\frac{1}{2}} + O(\lambda^{\frac{1}{2}})$, where

$$C_{\boldsymbol{\alpha}} = \left(\sum_{i=0}^{p-1} \alpha_i \log \alpha_i^{-1} \right)^{-1}.$$

(3) if $\langle \boldsymbol{\alpha} \rangle > 1$ ($d_s > 1$), there exists a bounded function $\rho^{\infty}_{\mathfrak{a}}(\lambda)$, s.t.

$$\rho_{\mathfrak{a}} = \rho^{\infty}_{\mathfrak{a}}(\lambda)\, \lambda^{\frac{d_s}{2}} + o(\lambda^{\frac{d_s}{2}}), \quad \mathfrak{a} \in \{\mathfrak{d}, \mathfrak{n}\}, \tag{4.8}$$

where the function $\rho^{\infty}_{\mathfrak{a}}(\lambda)$ satisfies the following:

- *if $\gamma_j = \log \alpha_j^{-1}$ form an arithmetic set (i.e. $\gamma_j/\gamma_k \in \mathbb{Q}$ for all j, k), then $\rho^{\infty}_{\mathfrak{a}}(\lambda) = \psi^{\infty}_{\mathfrak{a}}(\log \lambda)$ with $\psi^{\infty}_{\mathfrak{a}}$ piecewise-continuous and periodic, s.t.*

$$0 < c < \psi^{\infty}_{\mathfrak{a}}(\lambda) < C, \quad \lambda > 0.$$

- *otherwise (in a general case), $\rho^{\infty}_{\mathfrak{a}}(\lambda) = \mathrm{const} > 0$.*

The proof of this theorem relies on two main ingredients, used previously in the eigenvalue analysis on fractals: a recursive equation for $\rho_{\mathfrak{a}}(\lambda)$ and the renewal theory [7], [16] (see Section 4.2.2).

4.2.1. *A recursive equation for $\rho_{\mathfrak{a}}(\lambda)$.* This section is dedicated to the proof of the recursive equation for $\rho_{\mathfrak{a}}(\lambda)$. For this, we will extensively use the well-known min-max characterization of the eigenvalues:

$$\mathcal{F}^n(V_{\mathfrak{a}}) := \{Q :\ Q \subset V_{\mathfrak{a}}, \quad \dim Q = n\},$$

$$\omega^2_{\mathfrak{a},n} = \inf_{Q \in \mathcal{F}^n(V_{\mathfrak{a}})} \sup_{v \in Q} \frac{a(v,v)}{\|v\|^2_{\mathrm{L}^2_\mu(\mathcal{T})}}. \tag{4.9}$$

Lemma 4.9 (A recursive equation)**.** *The functions* $\rho_{\mathfrak{a}}(\lambda)$, $\mathfrak{a} \in \{\mathfrak{n}, \mathfrak{d}\}$ *satisfy*

$$\rho_{\mathfrak{a}}(\lambda) = r_{\mathfrak{a}}(\lambda) + \sum_{j=0}^{p-1} \rho_{\mathfrak{a}}(\alpha_j^2 \lambda), \qquad \lambda \geq 0, \tag{4.10}$$

where $r_{\mathfrak{a}}(\lambda)$ *is a piecewise-continuous function, s.t.*

$$\lfloor \pi^{-1}\sqrt{\lambda} \rfloor \leq r_{\mathfrak{a}}(\lambda) \leq \lfloor \pi^{-1}\sqrt{\lambda} \rfloor + p + 1. \tag{4.11}$$

Moreover, there exists $\lambda_* > 0$*, s.t.* $r_{\mathfrak{a}}(\lambda) = 0$ *and* $\rho_{\mathfrak{a}}(\lambda) = 0$ *for* $\lambda < \lambda_*$*.*

Proof. We will prove the respective result for $\rho_{\mathfrak{n}}(\lambda) \equiv \rho_{\mathfrak{n}}(\lambda; \mathcal{T})$, the proof for $\rho_{\mathfrak{d}}(\lambda)$ being almost verbatim the same. It is based on two ideas: the classical Dirichlet-Neumann bracketing technique [14] and a rescaling argument.
Step 1. Dirichlet-Neumann bracketing.
Step 1.1. Auxiliary spaces and counting functions. Let us introduce the following auxiliary spaces and counting functions. First, we define an operator $\mathcal{A}_N$ associated to the sesquilinear form $a(u, v)$ (3.1), defined like $\mathcal{A}_{\mathfrak{a}}$ in (3.2), but with the domain (remark that $V_{\mathfrak{a}}$ is replaced by $\mathrm{H}^1_\mu(\mathcal{T})$):

$$\mathcal{D}(\mathcal{A}_N; \mathcal{T}) = \{u \in \mathrm{H}^1_\mu(\mathcal{T}) : \ |a(u, v)| \leq C(u)\|v\|_{\mathrm{L}^2_\mu(\mathcal{T})}, \quad \forall v \in \mathrm{H}^1_\mu(\mathcal{T})\}.$$

The associated counting function will be denoted by $\rho_N(\lambda; \mathcal{T})$, and the set of all the eigenvalues of $\mathcal{A}_N$ by $\sigma_N(\mathcal{T})$.
Denoting by $\mathcal{T}(\Sigma_{1,j})$ the self-similar p-adic tree whose root edge is $\Sigma_{1,j}$, we introduce the following broken space

$$\widetilde{V}_N(\mathcal{T}) := \{u \in \mathrm{L}^2_\mu(\mathcal{T}) : \ u|_{\Sigma_{0,0}} \in H^1(\Sigma_{0,0}),\ u(M^*) = 0,\ u|_{\mathcal{T}(\Sigma_{1,j})} \in \mathrm{H}^1_\mu(\mathcal{T}(\Sigma_{1,j}))\}.$$

See Figure 2 for an illustration. We will denote by $\widetilde{\sigma}_N$ the spectrum and by $\widetilde{\rho}_N(\lambda)$ the associated counting function of the operator $\widetilde{\mathcal{A}}_N$, defined like in (3.2), with the domain

$$\mathcal{D}(\widetilde{\mathcal{A}}_N) = \{u \in \widetilde{V}_N(\mathcal{T}) : \ |a(u, v)| \leq C(u)\|v\|_{\mathrm{L}^2_\mu(\mathcal{T})}, \quad \forall v \in \widetilde{V}_N(\mathcal{T})\}.$$

Finally, let

$$\widetilde{V}_{\mathfrak{n}}(\mathcal{T}) = \{v \in V_{\mathfrak{n}}(\mathcal{T}) : \ v(M_{0,0}) = 0\},$$

see Figure 2 for an illustration. The spectrum of the associated operator $\widetilde{\mathcal{A}}_{\mathfrak{n}}$ will be denoted by $\widetilde{\sigma}_{\mathfrak{n}}$, and the counting function by $\widetilde{\rho}_{\mathfrak{n}}(\lambda)$.

Step 1.2. Relations between the counting functions.
Relating $\rho_{\mathfrak{n}}(\lambda)$ *and* $\rho_N(\lambda; \mathcal{T})$*.* We will need an upper bound for ρ_N in terms of $\rho_{\mathfrak{n}}$. It can be obtained from the same arguments as [14, Corollary 4.7]. Namely,

$$\rho_N(\lambda; \mathcal{T}) \leq \rho_{\mathfrak{n}}(\lambda) + \dim\left(\mathrm{H}^1_\mu(\mathcal{T}) \setminus V_{\mathfrak{n}}(\mathcal{T})\right) = \rho_{\mathfrak{n}}(\lambda) + 1. \tag{4.12}$$

Relating $\rho_{\mathfrak{n}}(\lambda)$ *and* $\widetilde{\rho}_N(\lambda)$*.* Thanks to the min-max principle (4.9), because $V_{\mathfrak{n}}(\mathcal{T}) \subset \widetilde{V}_N(\mathcal{T})$, we obtain

$$\rho_{\mathfrak{n}}(\lambda) \leq \widetilde{\rho}_N(\lambda). \tag{4.13}$$

Relating $\rho_{\mathfrak{n}}(\lambda)$ *and* $\widetilde{\rho}_{\mathfrak{n}}(\lambda)$*.* Because $\widetilde{V}_{\mathfrak{n}}(\mathcal{T}) \subset V_{\mathfrak{n}}(\mathcal{T})$, we obtain, by the min-max principle,

$$\rho_{\mathfrak{n}}(\lambda) \geq \widetilde{\rho}_{\mathfrak{n}}(\lambda). \tag{4.14}$$

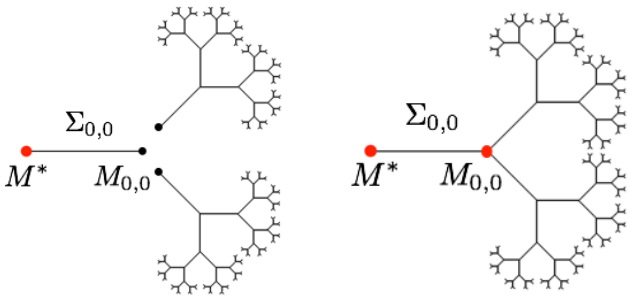

FIGURE 2. Left: we illustrate the space $\widetilde{V}_N(\mathcal{T})$, which includes functions that may be discontinuous in the point $M_{0,0}$. Right: an illustration to the space $\tilde{V}_{\mathfrak{n}}(\mathcal{T})$, where all functions vanish in the point $M_{0,0}$. By red we mark the points where the functions vanish.

Step 2. An equation for $\widetilde{\rho}_N(\lambda)$.
Step 2.1. An immediate identity. Because, with an obvious abuse of notation,

$$\widetilde{V}_N = V_{\mathfrak{n}}(\Sigma_{0,0}) \oplus \bigoplus_{j=0}^{p-1} \mathrm{H}^1_\mu(\mathcal{T}(\Sigma_{1,j})),$$
$$\text{where } V_{\mathfrak{n}}(\Sigma_{0,0}) := \{u \in H^1(\Sigma_{0,0}) : u(M^*) = 0\},$$

the spectrum $\widetilde{\sigma}_N$ of $\widetilde{\mathcal{A}}_N$ consists of the eigenvalues of $-\Delta$ on $V_{\mathfrak{n}}(\Sigma_{0,0})$ (the associated counting function is denoted by $\rho_{\mathfrak{n}}(\lambda;\Sigma_{0,0})$ and is explicitely known) and the union

$$\bigcup_{j=0}^{p-1} \sigma_N(\mathcal{T}(\Sigma_{1,j}))).$$

Thus the counting function $\widetilde{\rho}_N$ is a sum of the respective counting functions

$$\widetilde{\rho}_N(\lambda) = \rho_{\mathfrak{n}}(\lambda;\Sigma_{0,0}) + \sum_{j=0}^{p-1} \rho_N(\lambda;\mathcal{T}(\Sigma_{1,j})), \quad \rho_{\mathfrak{n}}(\lambda;\Sigma_{0,0}) = \left\lfloor \pi^{-1}\lambda^{\frac{1}{2}} + \frac{1}{2} \right\rfloor. \tag{4.15}$$

Step 2.2. Scaling argument. The goal of this step is to show that the counting function $\rho_N(\lambda;\mathcal{T}(\Sigma_{1,j}))$ satisfies:

$$\rho_N(\lambda;\mathcal{T}(\Sigma_{1,j})) = \rho_N(\alpha_j^2\lambda;\mathcal{T}). \tag{4.16}$$

To see this, we get back to the min-max characterization of eigenvalues (4.9). In particular, since $\mathcal{T}(\Sigma_{1,j})$ is obtained from $\mathcal{T}$ by a similitude transformation γ_j of the ratio α_j (cf. [10]), we obtain the following identities, valid for any $v \in \mathrm{H}^1_\mu(\mathcal{T})$,

$$\int_{\mathcal{T}} |v(s)|^2 \mu ds = \mu_j^{-1} \int_{\mathcal{T}(\Sigma_{1,j})} |v(\gamma_j^{-1}(\tilde{s}))|^2 \, \alpha_j^{-1} \, \mu(\tilde{s}) \, d\tilde{s},$$
$$\int_{\mathcal{T}} |\partial_s v(s)|^2 \mu ds = \mu_j^{-1} \int_{\mathcal{T}(\Sigma_{1,j})} |\partial_{\tilde{s}} v(\gamma_j^{-1}(\tilde{s}))|^2 \, \alpha_j \, \mu(\tilde{s}) \, d\tilde{s},$$

and thus, see the min-max principle (4.9),

$$\omega_{N,\ell}^2 \in \sigma_N(\mathcal{T}) \iff \alpha_j^{-2}\omega_{N,\ell}^2 \in \sigma_N(\mathcal{T}(\Sigma_{1,j})). \tag{4.17}$$

The above gives (4.16).

Step 2.3. Summary. Combining (4.16) with (4.15), we obtain

$$\widetilde{\rho}_N(\lambda) = \left\lfloor \pi^{-1}\lambda^{\frac{1}{2}} + \frac{1}{2} \right\rfloor + \sum_{j=0}^{p-1} \rho_N(\alpha_j^2\lambda; \mathcal{T}). \tag{4.18}$$

Step 3. An equation for $\widetilde{\rho}_{\mathfrak{n}}(\lambda)$.
Just like in the previous case, we remark that (with an abuse of notation)

$$\widetilde{V}_{\mathfrak{n}} = H_0^1(\Sigma_{0,0}) \oplus \bigoplus_{j=0}^{p-1} V_{\mathfrak{n}}(\mathcal{T}(\Sigma_{1,j})).$$

Repeating the same arguments as in Step 2, we get the recursive equation for $\widetilde{\rho}_{\mathfrak{n}}(\lambda)$:

$$\widetilde{\rho}_{\mathfrak{n}}(\lambda) = \lfloor \pi^{-1}\lambda^{\frac{1}{2}} \rfloor + \sum_{j=0}^{p-1} \rho_{\mathfrak{n}}(\alpha_j^2\lambda). \tag{4.19}$$

Step 4. Proof of (4.10).
Combining (4.18) with the inequality $\rho_{\mathfrak{n}} \le \widetilde{\rho}_N$, cf. (4.13),

$$\begin{aligned} \rho_{\mathfrak{n}}(\lambda) &\le \left\lfloor \pi^{-1}\lambda^{\frac{1}{2}} + \frac{1}{2} \right\rfloor + \sum_{j=0}^{p-1} \rho_N(\alpha_j^2\lambda; \mathcal{T}) \\ &\le \left\lfloor \pi^{-1}\lambda^{\frac{1}{2}} + \frac{1}{2} \right\rfloor + \sum_{j=0}^{p-1} \rho_{\mathfrak{n}}(\alpha_j^2\lambda) + p, \end{aligned} \tag{4.20}$$

where the last bound was obtained from (4.12).

To get the lower bound, we combine the inequality $\rho_{\mathfrak{n}} \ge \widetilde{\rho}_{\mathfrak{n}}$, cf. (4.14), and (4.19):

$$\rho_{\mathfrak{n}}(\lambda) \ge \left\lfloor \pi^{-1}\lambda^{\frac{1}{2}} \right\rfloor + \sum_{j=0}^{p-1} \rho_{\mathfrak{n}}(\alpha_j^2\lambda). \tag{4.21}$$

From (4.20) and (4.21) we see that, setting $r_{\mathfrak{n}}(\lambda) := \rho_{\mathfrak{n}}(\lambda) - \sum_{j=0}^{p-1} \rho_{\mathfrak{n}}(\alpha_j^2\lambda)$,

$$\left\lfloor \pi^{-1}\lambda^{\frac{1}{2}} \right\rfloor \le r_{\mathfrak{n}}(\lambda) \le \left\lfloor \pi^{-1}\lambda^{\frac{1}{2}} \right\rfloor + p + 1.$$

This proves (4.10). Note that $r_{\mathfrak{n}}(\lambda)$ inherits piecewise-continuity from $\rho_{\mathfrak{n}}(\lambda)$.

Step 5. 'Causality' of $\rho_{\mathfrak{n}}(\lambda)$, $r_{\mathfrak{n}}(\lambda)$. Since $\omega = 0$ is not an eigenvalue of $\mathcal{A}_{\mathfrak{n}}$, see the discussion after (3.3), there exists $\lambda_* > 0$, s.t. $\rho_{\mathfrak{n}}(\lambda) = 0$ for $\lambda \in (0, \lambda_*)$; same holds for $\rho_{\mathfrak{n}}(\alpha_j^2\lambda)$, for $j = 0, \dots, p-1$, since $\alpha_j < 1$. Therefore, $r_{\mathfrak{n}}(\lambda) = 0$ for $\lambda < \lambda_*$. □

4.2.2. *Renewal theorem.* To handle the equation (4.10), we will use the renewal theorem, cf. [7, p. 358] or [13, Appendix B.4]; we will exploit its version suggested by Levitin, Vassiliev [16], whose statement is the most suitable for our needs.

Theorem 4.10 (Renewal theorem, [16]). *Let $\psi : \mathbb{R} \to \mathbb{R}$ satisfy*

$$\psi(x) = \Psi(x) + \sum_{j=0}^{p-1} c_j \psi(x - \gamma_j), \quad c_j, \gamma_j > 0,\ j = 0, \dots, p-1, \quad \sum_{j=0}^{p-1} c_j = 1. \tag{4.22}$$

Here Ψ is a piecewise-continuous function on $\mathbb{R}$, s.t. $|\Psi(x)| < C\mathrm{e}^{-\tau|x|}$, C, $\tau \geq 0$. Assume additionally $\psi(x) \to 0$, as $x \to -\infty$. Then

- *ψ is uniformly bounded on $\mathbb{R}$.*
- *moreover, as $x \to +\infty$,*

$$\psi(x) = \psi_\infty(x) + o(1),$$

where $\psi_\infty(x)$ is a periodic function defined as follows:

(1) if the set γ_j is arithmetic (i.e. $\gamma_j/\gamma_k \in \mathbb{Q}$ for all j, k), then

$$\psi_\infty(x) = \gamma J^{-1} \sum_{k=-\infty}^{\infty} \Psi(x - k\gamma),$$

where $J = \sum_{j=0}^{p-1} c_j \gamma_j$ and γ is the largest number s.t. $\frac{\gamma_j}{\gamma} \in \mathbb{Z}$ for all j.

(2) otherwise,

$$\psi_\infty(x) = \mathrm{const} = J^{-1} \int_{-\infty}^{\infty} \Psi(x)dx.$$

We will use the direct consequence of Theorem 4.10, item 1, formulated below.

Lemma 4.11. *Let $\varphi : \mathbb{R}^+ \to \mathbb{R}$ satisfy*

$$\varphi(\lambda) = \Phi(\lambda) + \sum_{j=0}^{p-1} \varphi(\alpha_j^2 \lambda), \tag{4.23}$$

where Φ is a piecewise-continuous function on $\mathbb{R}^+$, s.t. for some $C_\Phi > 0$ and $\delta > 0$, with d_s like in (4.5),

$$|\Phi(\lambda)| \leq C_\Phi \lambda^{\frac{d_s - \delta}{2}}, \qquad \text{for all } \lambda > 0. \tag{4.24}$$

Let additionally $\varphi(\lambda)$, $\Phi(\lambda)$ vanish for $\lambda \leq \lambda_*$, where $\lambda_* > 0$.

Then, there exists $C > 0$, s.t. for all $\lambda > 0$, $|\varphi(\lambda)| \leq C\lambda^{\frac{d_s}{2}}$, .

Proof. The proof follows closely the proof of Lemma 2.2 in [16]. We will rewrite (4.23) in the form required by Theorem 4.10, by change of variables and rescaling. First of all, the change of variables $x := \frac{1}{2}\log\lambda$, $\lambda > 0$, in (4.23) results in

$$\varphi(\mathrm{e}^{2x}) = \Phi(\mathrm{e}^{2x}) + \sum_{j=0}^{p-1} \varphi(\alpha_j^2 \mathrm{e}^{2x}) = \Phi(\mathrm{e}^{2x}) + \sum_{j=0}^{p-1} \varphi(\mathrm{e}^{2(x - \log \alpha_j^{-1})}). \tag{4.25}$$

It remains to make appear the weights c_j required in (4.22). For this we multiply (4.25) by $\mathrm{e}^{-d_s x}$ and set $\psi(x) = \varphi(\mathrm{e}^{2x})\mathrm{e}^{-d_s x}$. This gives

$$\begin{aligned}\psi(x) &= \Phi(\mathrm{e}^{2x})\mathrm{e}^{-d_s x} + \sum_{j=0}^{p-1} \psi(\mathrm{e}^{2(x-\log\alpha_j^{-1})})\mathrm{e}^{-d_s \log\alpha_j^{-1}} \\ &= \Phi(\mathrm{e}^{2x})\mathrm{e}^{-d_s x} + \sum_{j=0}^{p-1} \alpha_j^{d_s}\psi(\mathrm{e}^{2(x-\log\alpha_j^{-1})}). \qquad (4.26)\end{aligned}$$

It remains to apply Theorem 4.10; first we need to verify that its conditions are satisfied:

- $\sum_{j=0}^{p-1} \alpha_j^{d_s} = 1$ by definition of d_s, see (4.5);
- $\Psi(x) := \Phi(\mathrm{e}^{2x})\mathrm{e}^{-d_s x}$ is piecewise-continuous, since Φ is piecewise-continuous;
- the bound $|\Psi(x)| \le C\mathrm{e}^{-\tau|x|}$ holds true (with $\tau = \delta > 0$) because
  - for $x < \frac{1}{2}\log\lambda_*$, $\Psi(x) = 0$;
  - for $x > 0$, $|\Psi(x)| \le C_\Phi\, \mathrm{e}^{-\delta x}$ is a direct consequence of (4.24);
  - if $\lambda_* < 1$, for $x \in \left[\frac{1}{2}\log\lambda_*,\, 0\right]$, $|\Psi(x)| \le C$, because $\Phi(\mathrm{e}^{2x})$ is bounded by a constant in this case.
- $\psi(x) \to 0$ as $x \to -\infty$, since $\varphi(\mathrm{e}^{2x}) = 0$ for $x < \frac{1}{2}\log\lambda_*$.

By Theorem 4.10, $\psi(x)$ is uniformly bounded on $\mathbb{R}$, and so is $\varphi(\lambda)\lambda^{-\frac{d_s}{2}}$, which proves that $|\varphi(\lambda)| \le c\lambda^{\frac{d_s}{2}}$. □

4.2.3. *Proof of Theorem 4.8.* Let us first explain the principal idea behind the proof of Theorem 4.8.

Main idea. To 'guess' the asymptotic bounds stated in Theorem 4.8, one can first formally assume that $\rho_{\mathfrak{a}}(\lambda) = C\lambda^\kappa + o(\lambda^\kappa)$, where κ is a power to be determined; with (4.10), this leads to the following equation as $\lambda \to \infty$:

$$C\lambda^\kappa + o(\lambda^\kappa) = \frac{\sqrt{\lambda}}{\pi} + o(1) + C\sum_{j=0}^{p-1} \alpha_j^{2\kappa}\lambda^\kappa + o(\lambda^\kappa),$$

or, alternatively,

$$C\left(1 - \sum_{j=0}^{p-1} \alpha_j^{2\kappa}\right)\lambda^\kappa = \frac{\sqrt{\lambda}}{\pi} + o(\lambda^\kappa).$$

The above shows that we should expect $\kappa \ge \frac{1}{2}$. In particular, $\kappa > \frac{1}{2}$ requires that

$$\sum_{j=0}^{p-1} \alpha_j^{2\kappa} = 1$$

(i.e. $2\kappa = d_s > 1$, which is possible only if $\langle\boldsymbol{\alpha}\rangle > 1$). On the other hand, $\kappa = \frac{1}{2}$ implies

$$C = \frac{1}{\pi} + C\sum_{j=0}^{p-1} \alpha_j,$$

from where we obtain $C = (1-\langle\boldsymbol{\alpha}\rangle)^{-1}$ (which is well-defined when $\langle\boldsymbol{\alpha}\rangle < 1$). Let us now prove the above rigorously. Let us remark that the proofs of the cases $\langle\boldsymbol{\alpha}\rangle \leq 1$ and $\langle\boldsymbol{\alpha}\rangle > 1$ slightly differ.

Case $\langle\boldsymbol{\alpha}\rangle < 1$. Let us remark that this case, though in a somewhat different setting, had been treated by Levitin and Vassiliev, cf. [16]. We nonetheless present its proof for completeness. Let, with $C_{\boldsymbol{\alpha}} = \pi^{-1}\left(1 - \langle\boldsymbol{\alpha}\rangle\right)^{-1}$,

$$\varphi_{\mathfrak{a}}(\lambda) := \rho_{\mathfrak{a}}(\lambda) - \left\lfloor C_{\boldsymbol{\alpha}}\lambda^{\frac{1}{2}} \right\rfloor.$$

Let us show that $\varphi_{\mathfrak{a}}(\lambda)$ satisfies the conditions of Lemma 4.11 (i.e. $\varphi = \varphi_{\mathfrak{a}}$ in Lemma 4.11). For this let us examine the difference

$$\Phi_{\mathfrak{a}}(\lambda) := \varphi_{\mathfrak{a}}(\lambda) - \sum_{j=0}^{p-1} \varphi_{\mathfrak{a}}(\alpha_j^2\lambda). \tag{4.27}$$

Because $\varphi_{\mathfrak{a}}(\lambda)$ is piecewise-continuous, and vanishes for $\lambda < \lambda_{**}$, with some $\lambda_{**} > 0$, it remains to show that $|\Phi_{\mathfrak{a}}(\lambda)| \leq C_\Phi \lambda^{\frac{d_s-\delta}{2}}$, for some $\delta > 0$. We will demonstrate the uniform bound $|\Phi_{\mathfrak{a}}(\lambda)| \leq C_\Phi$.

Let us prove the lower bound $\Phi_{\mathfrak{a}} \geq -C_\Phi$. By Lemma 4.9, (4.10),

$$\Phi_{\mathfrak{a}}(\lambda) = r_{\mathfrak{a}}(\lambda) + \sum_{j=0}^{p-1} \rho_{\mathfrak{a}}(\alpha_j^2\lambda) - \left\lfloor C_{\boldsymbol{\alpha}}\lambda^{\frac{1}{2}} \right\rfloor - \sum_{j=0}^{p-1} \left(\rho_{\mathfrak{a}}(\alpha_j^2\lambda) - \left\lfloor C_{\boldsymbol{\alpha}}\alpha_j\lambda^{\frac{1}{2}} \right\rfloor \right).$$

Using $x \geq \lfloor x \rfloor \geq x - 1$ and the bounds of Lemma 4.9,

$$\Phi_{\mathfrak{a}}(\lambda) \geq \pi^{-1}\sqrt{\lambda} - 1 - C_{\boldsymbol{\alpha}}\lambda^{\frac{1}{2}} + \sum_{j=0}^{p-1} \alpha_j C_{\boldsymbol{\alpha}}\lambda^{\frac{1}{2}} - p.$$

Thus, with $C_{\boldsymbol{\alpha}} = \pi^{-1}(1 - \langle\boldsymbol{\alpha}\rangle)^{-1}$, $\Phi_{\mathfrak{a}}(\lambda) \geq -1 - p$. The upper bound can be obtained repeating the same arguments almost verbatim.

Applying Lemma 4.11, we deduce that $\varphi_{\mathfrak{a}}(\lambda)$ is bounded, and hence the conclusion about $\varphi_{\mathfrak{a}}(\lambda) = O(\lambda^{\frac{d_s}{2}})$, $d_s < 1$.

Case $\langle\boldsymbol{\alpha}\rangle = 1$. The proof mimics the proof of the case $\langle\boldsymbol{\alpha}\rangle < 1$ almost verbatim, with the only difference being that the function under consideration is

$$\varphi_{\mathfrak{a}}(\lambda) = \rho_{\mathfrak{a}}(\lambda) - \left\lfloor \pi^{-1} \left(\sum_{i=0}^{p-1} \alpha_i \log \alpha_i^{-1} \right)^{-1} \lambda^{\frac{1}{2}} \log \lambda^{\frac{1}{2}} \right\rfloor.$$

We leave the details to the reader.

Case $\langle\boldsymbol{\alpha}\rangle > 1$. In this case we will not apply Lemma 4.11, but rather use a refined result stated in the end of Theorem 4.10.

For this we rewrite the recursive relation (4.10) like in the proof of Lemma 4.11, cf. (4.26). With $\psi_{\mathfrak{a}}(x) = \rho_{\mathfrak{a}}(\mathrm{e}^{2x})\mathrm{e}^{-d_s x}$, (4.10) gives

$$\psi_{\mathfrak{a}}(x) = r_{\mathfrak{a}}(\mathrm{e}^{2x})\mathrm{e}^{-d_s x} + \sum_{j=0}^{p-1} \psi(x - \log \alpha_j^{-1})\alpha_j^{d_s}.$$

Remark that the equation satisfies the conditions of Theorem 4.10 (this can be shown using the same arguments as in the proof of Lemma 4.11, using $r_{\mathfrak{a}}(\mathrm{e}^{2x}) \leq$

Ce^x and $d_s > 1$). Thus we can apply Theorem 4.10 item 2, which results in the desired statement about the asymptotic behaviour of $\rho_{\mathfrak{a}}(\lambda)$. Let us remark that the periodicity of $\psi^\infty_{\mathfrak{a}}(x)$ follows directly from its explicit expression in Theorem 4.10, statement 2. Its boundedness is a consequence of Theorem 4.10 item 1. Moreover, $\psi^\infty_{\mathfrak{a}}$ is strictly positive: in the non-arithmetic case this follows immediately from its explicit expression, while in the arithmetic case we recall that (with the notation of Theorem 4.10)

$$\psi^\infty_{\mathfrak{a}}(x) = \gamma J^{-1} \sum_{k=-\infty}^{\infty} r_{\mathfrak{a}}(\mathrm{e}^{2x-2k\gamma})\mathrm{e}^{-d_s(x-k\gamma)} \geq \gamma J^{-1} \sum_{k=-\infty}^{0} r_{\mathfrak{a}}(\mathrm{e}^{2x-2k\gamma})\mathrm{e}^{-d_s(x-k\gamma)},$$

where the last inequality holds true because $r_{\mathfrak{a}}$ is non-negative. From the explicit expression for $r_{\mathfrak{a}}$ in (4.11) we see that for all sufficiently large x the above is strictly positive, and therefore, by periodicity of $\psi^\infty_{\mathfrak{a}}$, $\psi^\infty_{\mathfrak{a}}(x) > 0$ for all $x > 0$. □

4.2.4. *Numerical experiments: sharpness of the bounds.* In this section we compute numerically the quantity (cf. (4.4) for the definition of $\mathcal{P}_{\mathfrak{a}}$)

$$N_{\mathfrak{a}}(\lambda) := \#\{n : \widetilde{\omega}^2_{\mathfrak{a},n} < \lambda, \quad \widetilde{\omega}_{\mathfrak{a},n} \in \mathcal{P}_{\mathfrak{a}}\}, \tag{4.28}$$

which corresponds to the number of positive poles of $\mathbf{\Lambda}_{\mathfrak{a}}(\omega)$ not exceeding $\sqrt{\lambda}$. We compare it to the theoretical bounds for the respective counting function $\rho_{\mathfrak{a}}(\lambda)$, obtained in Theorem 4.8. By (4.4), $N_{\mathfrak{a}}(\lambda) \equiv N_{\mathfrak{a},\varepsilon}$ with $\varepsilon = \lambda^{-\frac{1}{2}}$.
The poles of $\mathbf{\Lambda}_{\mathfrak{a}}(\omega)$ are computed with the numerical method briefly outlined in Section 5.3. We consider multiple cases:

(1) Case 1 of Theorem 4.8, i.e. $d_s < 1$. Again, we study two sub-cases:

- $\boldsymbol{\alpha} = (0.5, 0.2)$, $\boldsymbol{\mu} = (1, 2)$, cf. Figure 3, left. We observe a good agreement with the asymptotics of Theorem 4.8. Let us remark that a small difference in this asymptotics (which is more visible for the Dirichlet case) can be attributed to the fact that the second-order term in the asymptotic expansion of $\rho_{\mathfrak{a}}(\lambda)$ is $O(\lambda^{\frac{d_s}{2}})$, with $d_s \approx 0.64$. This may be non-negligible with respect to $\sqrt{\lambda}$ for the values of λ considered.

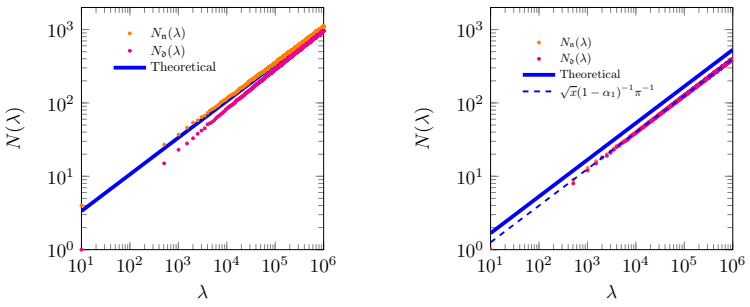

FIGURE 3. $N_{\mathfrak{a}}(\lambda)$ vs asymptotics for $\rho_{\mathfrak{a}}(\lambda)$ (given by Theorem 4.8) for the case when $\langle\boldsymbol{\alpha}\rangle < 1$. Left: $\boldsymbol{\alpha} = (0.5, 0.2)$ and $\boldsymbol{\mu} = (1, 2)$. Right: $\boldsymbol{\alpha} = (0.2, 0.2)$ and $\boldsymbol{\mu} = (1, 2)$. In this case the difference between $N_{\mathfrak{d}}$ and $N_{\mathfrak{n}}$ is not visible on the plot scale.

- $\boldsymbol{\alpha} = (0.2, 0.2)$, $\boldsymbol{\mu} = (1, 2)$, cf. Figure 3, right. In this case Theorem 4.8 does not seem to provide a correct asymptotics for $N_{\mathfrak{a}}(\lambda)$. In numerical experiments, we observe
$$N_{\mathfrak{a}}(\lambda) = (1-\alpha_1)^{-1}\pi^{-1}\lambda^{\frac{1}{2}} + o(\lambda^{\frac{1}{2}}),$$
instead of $N_{\mathfrak{a}}(\lambda) = (1-2\alpha_1)^{-1}\pi^{-1}\lambda^{\frac{1}{2}} + o(\lambda^{\frac{1}{2}})$.
This discrepancy is due to two phenomena. First of all, it can be proven rigorously that in the case of a symmetric tree, there exist eigenvalues ω_n, s.t. the corresponding eigenfunctions φ_n satisfy $\partial_s\varphi_n(M^*) = 0$ (i.e. they vanish on the root branch of the tree), and thus the corresponding coefficients a_n in the expansion (3.5) vanish. These eigenfunctions correspond to eigenvalues of high multiplicity.
Second, in general, there may exist eigenvalues of high multiplicity, s.t. the corresponding eigenfunctions φ_n satisfy $\partial_s\varphi_n(M^*) \neq 0$. These eigenvalues are counted with their multiplicity in $\rho_{\mathfrak{a}}(\lambda)$, which is not the case for $N_{\mathfrak{a}}(\lambda)$.
Let us remark that in the case of the symmetric tree, the fact that $N_{\mathfrak{a}}(\lambda) \neq \rho_{\mathfrak{a}}(\lambda)$ can be proven rigorously by examining the non-linear equation (4.29): its solution $\boldsymbol{\Lambda}(\omega)$ corresponding to $p = 2$, (α_1, α_1) and (μ_1, μ_2) coincides with the solution $\boldsymbol{\Lambda}(\omega)$ corresponding to $p = 1$, $\alpha = \alpha_1$ and $\mu = \mu_1 + \mu_2$ (and then we can bound $N_{\mathfrak{a}}$ by $\rho_{\mathfrak{a}}$ corresponding to this, latter, tree).

(2) Case 2 of Theorem 4.8, i.e. $d_s = 1$. The numerical experiment for the case $\boldsymbol{\alpha} = (0.4, 0.6)$, $\boldsymbol{\mu} = (0.5, 0.3)$, cf. Figure 4, left, indicates a good agreement of the asymptotic behaviour of $N_{\mathfrak{d}}(\lambda)$ with $\rho_{\mathfrak{d}}(\lambda)$. There is however a significant discrepancy in the behaviour of $N_{\mathfrak{n}}(\lambda)$ compared to the theoretical values of $\rho_{\mathfrak{n}}(\lambda)$. This can be explained by the fact that the second order term in the asymptotic expansion for $\rho_{\mathfrak{a}}(\lambda)$ is $O(\lambda^{\frac{1}{2}})$, which can be close to the principal asymptotics term $O(\lambda^{\frac{1}{2}}\log\lambda)$ for the values of λ under consideration.

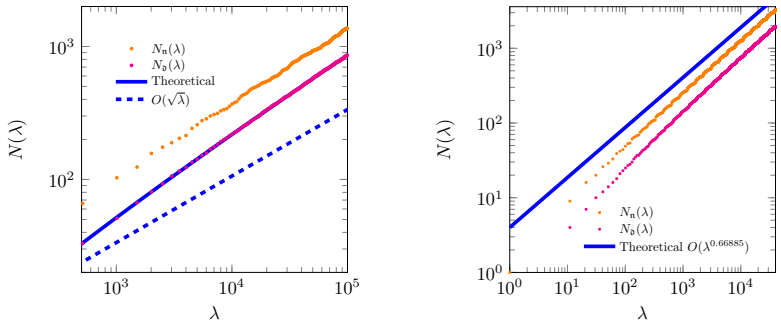

FIGURE 4. $N_{\mathfrak{a}}(\lambda)$ vs asymptotics for $\rho_{\mathfrak{a}}(\lambda)$ (given by Theorem 4.8) for the case when $\langle\boldsymbol{\alpha}\rangle \geq 1$. Left: $\boldsymbol{\alpha} = (0.6, 0.4)$ and $\boldsymbol{\mu} = (1, 0.5)$. Right: $\boldsymbol{\alpha} = (0.45, 0.73)$ and $\boldsymbol{\mu} = (0.5, 0.5)$.

(3) Case 3 of Theorem 4.8, when $d_s > 1$. We study multiple cases:

- the non-arithmetic case: $\boldsymbol{\alpha} = (0.45, 0.73)$, $\boldsymbol{\mu} = (0.5, 0.5)$. See Figure 4, right.
- the arithmetic case: $\boldsymbol{\alpha} = (0.64, 0.8)$, $\boldsymbol{\mu} = (0.5, 0.5)$. See Figure 5, left.

- a special case of the arithmetic configuration: a symmetric tree ($\alpha_i = \alpha_j$ for some $i \neq j$). We take $\boldsymbol{\alpha} = (0.8, 0.8)$, $\boldsymbol{\mu} = (0.4, 0.6)$. See Figure 5, right.

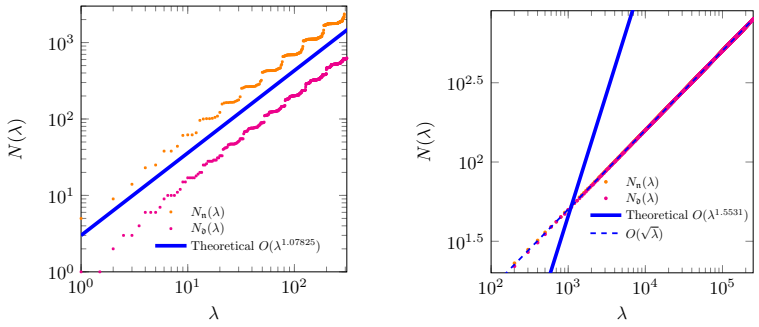

FIGURE 5. Comparison of $N_{\mathfrak{a}}(\lambda)$, $\mathfrak{a} \in \{\mathfrak{d}, \mathfrak{n}\}$ and asymptotics for $\rho_{\mathfrak{a}}(\lambda)$ deduced in Theorem 4.8 for different values of $\boldsymbol{\alpha}$, for the arithmetic cases. Left: $\boldsymbol{\alpha} = (0.64, 0.8)$, $\boldsymbol{\mu} = (0.5, 0.5)$. Right: $\boldsymbol{\alpha} = (0.8, 0.8)$, $\boldsymbol{\mu} = (0.4, 0.6)$. In the latter case, on the plot scale the difference between $N_{\mathfrak{d}}$ and $N_{\mathfrak{n}}$ is almost invisible.

Multiple phenomena can be observed:

- in the non-arithmetic and arithmetic cases, when the tree is not symmetric (Figure 4, right, and Figure 5, left), the behaviour of $N_{\mathfrak{a}}$ is in a good agreement with the asymptotic behaviour of $\rho_{\mathfrak{a}}(\lambda)$, i.e. $O(\lambda^{\frac{d_s}{2}})$, predicted by Theorem 4.8. In particular, we clearly observe the log-periodic behaviour of $N_{\mathfrak{a}}\lambda^{-\frac{d_s}{2}}$ in the arithmetic case.
- in the case of the symmetric tree (Figure 5, right), however, we observe a large discrepancy in the asymptotic powers. Numerically, $N_{\mathfrak{a}}(\lambda) = O\left(\lambda^{\frac{1}{2}}\right)$, while $\rho_{\mathfrak{a}}(\lambda) = O(\lambda^{\frac{d_s}{2}})$, with $d_s = \frac{\log 0.5}{\log 0.8} \approx 3.1063$. Again, just like in the symmetric case for $\langle \boldsymbol{\alpha} \rangle < 1$, cf. Figure 3, right, this can be explained by the presence of the eigenvalues of high multiplicity and the fact that the coefficients a_n in (3.5) may vanish for some values of n.

4.3. **Lower bound for $N_{\mathfrak{a},\varepsilon}$.** As we have demonstrated numerically in Section 4.2.4, an asymptotic distribution of the poles of $\boldsymbol{\Lambda}_{\mathfrak{a}}(\lambda)$ can be quite different from the asymptotic distribution of eigenvalues of the operator $\mathcal{A}_{\mathfrak{a}}$. The goal of this section is to provide a lower bound for $N_{\mathfrak{a}}(\lambda)$ (and, consequently, on $N_{\mathfrak{a},\varepsilon}$). The principal result of this section reads

Theorem 4.12. *For $\mathfrak{a} \in \{\mathfrak{n}, \mathfrak{d}\}$, $N_{\mathfrak{a}}(\lambda) \geq \left\lfloor \sqrt{\frac{\lambda}{2\pi}} \right\rfloor$.*

The above result does not follow from any of the bounds for the counting functions, obtained in Section 4.2, since it also encodes some information about the eigenfunctions. It shows that inside the interval $(0, \lambda)$ there are at least $O\left(\lambda^{\frac{1}{2}}\right)$ distinct eigenvalues, with corresponding eigenfunctions $\varphi_{\mathfrak{a}}$ satisfying $\partial_s \varphi_{\mathfrak{a}}(M^*) \neq 0$.

The proof of the above theorem is very simple, and relies on Lemma 5.3 from [10], which shows that $\mathbf{\Lambda}_{\mathfrak{a}}(\omega)$ satisfies a certain non-linear equation.

Lemma 4.13 (Lemma 5.3 from [10])**.** *For any $\omega \in \mathbb{C} \setminus \mathbb{R}$,*

$$\mathbf{\Lambda}_{\mathfrak{a}}(\omega) = -\omega \frac{\omega \tan \omega - \mathbf{F}_{\mathfrak{a}}(\omega)}{\tan \omega \mathbf{F}_{\mathfrak{a}}(\omega) + \omega}, \qquad \mathbf{F}_{\mathfrak{a}}(\omega) = \sum_{i=0}^{p-1} \frac{\mu_i}{\alpha_i} \mathbf{\Lambda}_{\mathfrak{a}}(\alpha_i \omega), \quad \mathfrak{a} \in \{\mathfrak{d}, \mathfrak{n}\}. \tag{4.29}$$

Another useful result is the monotonicity property for Herglotz functions, cf. [5].

Lemma 4.14. *For $\omega > 0$, s.t. ω is not a pole of $\mathbf{F}_{\mathfrak{a}}(\omega)$, $\mathbf{F}'_{\mathfrak{a}}(\omega) \leq 0$*

Proof. Let us show that for $\omega > 0$, $\mathbf{\Lambda}'_{\mathfrak{a}}(\omega) < 0$. This will immediately imply the desired result. Using the representation (3.5), cf. Theorem 3.1, we obtain

$$\mathbf{\Lambda}'_{\mathfrak{a}}(\omega) = -\sum_{n=0}^{+\infty} \frac{2 a_{\mathfrak{a},n} \omega \omega_{\mathfrak{a},n}^2}{(\omega_{\mathfrak{a},n}^2 - \omega^2)^2}.$$

It remains to notice that the above converges uniformly on compact subsets of $\mathbb{C}$ not containing the poles of $\mathbf{\Lambda}_{\mathfrak{a}}$ (this is easy to see by comparing the above series to the uniformly convergent series (3.5), cf. Theorem 3.1); moreover, the above quantity is negative for $\omega > 0$, since $a_{\mathfrak{a},n} \geq 0$ for all $n \geq 0$. □

The above two results suffice for the proof of Theorem 4.12.

Proof of Theorem 4.12. First, we will show that on each interval $I_m := [m\pi, (m+1)\pi]$, $m \in \mathbb{Z}$, the function $\mathbf{\Lambda}_{\mathfrak{a}}(\omega)$ has at least one pole. By evenness of $\mathbf{\Lambda}_{\mathfrak{a}}(\omega)$, we will consider $m \geq 0$.

Remark that $\omega = w_0$ ($\neq 0$) is a pole of $\mathbf{\Lambda}_{\mathfrak{a}}(\omega)$ iff either

(1) $\mathbf{F}_{\mathfrak{a}}(\omega)$ has a pole in w_0, and the denominator in (4.29) is continuous in w_0, i.e. $\tan w_0 = 0$. This implies in particular that $w_0 = k\pi$ for some $k \in \mathbb{N}$.
(2) $\tan \omega$ has a pole in w_0, and the denominator in (4.29) is continuous in w_0, i.e. $\mathbf{F}_{\mathfrak{a}}(\omega_0) = 0$. This implies in particular that $w_0 = (k + \frac{1}{2})\pi$ for some $k \in \mathbb{N}$.
(3) $\tan w_0 < \infty$, $\mathbf{F}_{\mathfrak{a}}(w_0) < \infty$, the denominator of (4.29) vanishes and the numerator does not, i.e.

$$\tan w_0 \mathbf{F}_{\mathfrak{a}}(w_0) = -w_0, \quad \text{and} \quad \mathbf{F}_{\mathfrak{a}}(w_0) \neq w_0 \tan w_0.$$

Remark that the first condition above implies the second one (as $-\frac{\omega}{\tan \omega} \neq \omega \tan \omega$ on $\mathbb{R}$), and thus the above reduces to

$$\mathbf{F}_{\mathfrak{a}}(w_0) = -\frac{w_0}{\tan w_0}.$$

Let us now assume that $\mathbf{\Lambda}_{\mathfrak{a}}(\omega)$ has no poles in I_m. In particular, this implies that

$$\mathbf{F}_{\mathfrak{a}}(\omega) \neq f(\omega), \quad f(\omega) = -\omega(\tan \omega)^{-1} \text{ on } I_m, \tag{4.30}$$

$$\mathbf{F}_{\mathfrak{a}} \text{ has no poles in } m\pi,\ (m+1)\pi. \tag{4.31}$$

It remains to consider two possibilities:

(1) $\mathbf{F}_{\mathfrak{a}}(\omega)$ has no poles on the interval I_m. By continuity of $\mathbf{F}_{\mathfrak{a}}(\omega)$ and $f(\omega)$ on $(m\pi,(m+1)\pi)$, (4.30) holds if and only if $\mathbf{F}_{\mathfrak{a}}(\omega) > f(\omega)$ or $\mathbf{F}_{\mathfrak{a}}(\omega) < f(\omega)$ on I_m. However, $f(\omega)$ is strictly growing on I_m, and

$$\lim_{\omega\to m\pi+} f(\omega) = -\infty, \qquad \lim_{\omega\to(m+1)\pi-} f(\omega) = +\infty.$$

Therefore $\mathbf{F}_{\mathfrak{a}}(\omega) > f(\omega)$ on I_m would mean that $\mathbf{F}_{\mathfrak{a}}(\omega)$ has a pole in $\omega = (m+1)\pi$, while $\mathbf{F}_{\mathfrak{a}}(\omega) < f(\omega)$ on I_m would imply that $\mathbf{F}_{\mathfrak{a}}(\omega)$ has a pole in $\omega = m\pi$ (which is a contradiction to (4.31)).

(2) $\mathbf{F}_{\mathfrak{a}}(\omega)$ has at least one pole inside I_m. We will consider the case when it has a single pole, while the case with several poles can be studied similarly.

Assume $\mathbf{F}_{\mathfrak{a}}(\omega)$ has a pole in $\omega = \omega_0 \in (m\pi,(m+1)\pi)$. By (4.30), on the interval $(m\pi,\omega_0)$, $\mathbf{F}_{\mathfrak{a}}(\omega) \neq f(\omega)$. This is possible iff the either of the conditions holds:

- on $(m\pi,\omega_0)$, $\mathbf{F}_{\mathfrak{a}}(\omega) > f(\omega)$. Let us show that this is impossible: by Lemma 4.14, $\mathbf{F}'_{\mathfrak{a}}(\omega) \leq 0$, and thus on the interval $(m\pi,\omega_0)$, $\mathbf{F}_{\mathfrak{a}}(\omega)$ is a continuous monotonically decreasing function that changes its value from $\mathbf{F}_{\mathfrak{a}}(m\pi)$ to $-\infty$. Because $f(\omega) = -\omega(\tan\omega)^{-1} < \mathbf{F}_{\mathfrak{a}}(\omega)$ is continuous in ω_0, this is impossible.
- on $(m\pi,\omega_0)$, $\mathbf{F}_{\mathfrak{a}}(\omega) < f(\omega)$, which is again impossible, because $f(\omega) \to -\infty$ as $\omega \to m\pi+$, but $\mathbf{F}_{\mathfrak{a}}(\omega)$ does not have a pole in $\omega = m\pi$.

Thus, there exists $\omega_* \in (m\pi,\omega_0)$, s.t. $\mathbf{F}_{\mathfrak{a}}(\omega_*) = -\omega_*(\tan\omega_*)^{-1}$, and we get a contradiction with (4.30).

Thus, inside each interval $[m\pi,(m+1)\pi]$ $\mathbf{\Lambda}_{\mathfrak{a}}(\omega)$ has at least one pole; hence, on each half-open interval $[m\pi,(m+2)\pi)$, $m \geq 0$, $\mathbf{\Lambda}_{\mathfrak{a}}(\omega)$ has at least one pole (we cannot guarantee that it has 2 poles, because the only pole could be $(m+1)\pi$); because the intervals of such form do not intersect, and the interval $(0,\lambda)$ contains at least $\lfloor\frac{\lambda}{2\pi}\rfloor$ such intervals (and thus poles), we conclude that $N_{\mathfrak{a}}(\lambda) \geq \left\lfloor\sqrt{\frac{\lambda}{2\pi}}\right\rfloor$. □

4.4. **Proof of Theorem 4.5.** The lower bound in Theorem 4.5 follows from the identity $N_{\mathfrak{a},\varepsilon} = N_{\mathfrak{a}}(\varepsilon^{-2})$ and Theorem 4.12. The upper bound follows from the bound $N_{\mathfrak{a},\varepsilon} \leq \rho_{\mathfrak{a}}(\varepsilon^{-2})$ and Theorem 4.8.

5. Numerical resolution of (3.15). Numerical experiments

In this section we address the numerical aspects of the resolution of (3.15). This section is organized as follows:

- in Section 5.1, we will present a stable discretization of (3.15).
- in Section 5.3 we will briefly outline our strategy to compute the poles and residues of $\mathbf{\Lambda}_{\mathfrak{a}}(\omega)$.
- Section 5.4 is dedicated to the numerical experiments.

5.1. **Discretization.** In this section we will discuss the discretization of (3.15). For this we will provide the discrete formulation and prove its stability; we will not address the convergence estimates, since they are not difficult (though, indeed, somewhat technical) to obtain, and can be proven using various Gronwall inequalities. We start with the semi-discretization in space, and then show a discretization in time.

5.1.1. *Semi-discretization in space.* Let $U_h \subset \mathrm{H}^1_\mu(\mathcal{T}^m)$ be an extension of the Lagrange P_1 space to the case of fractal trees, see [9] for the definition.

Provided $\dim U_h = N_s$, let $u_h = \sum_{k=0}^{N_s-1} u_k \varphi_k$ be an approximation to the exact solution u.

By $\mathbf{u}$ we will denote the coefficients $\mathbf{u} = (u_0, \dots, u_{N_s-1})$. The mass and stiffness matrices are denoted by $\mathbf{M}$ and $\mathbf{K}$ (remark that they are constructed with respect to the weighted $\mathrm{L}^2_\mu(\mathcal{T})$ product).

Let $\mathbf{P}$ be the discretization of the trace operator $\boldsymbol{\gamma}_m$:

$$\mathbf{P}_{j\ell} = \varphi_\ell(M_{m,j}).$$

Formulation. The discretization in space of (3.15a) reads:

find $u_{N,h} \in C^1([0,\, T]; U_h)$, s.t. $u_{N,h}(.,0) = \partial_t u_{N,h}(.,0) = 0$ and

$$(\partial_t^2 u_{N,h}, v_h)_{\mathcal{T}^m} + (\partial_s u_{N,h}, \partial_s v_h)_{\mathcal{T}^m} + \int_{\Gamma_m} \mathcal{B}_m^N(\partial_t) \boldsymbol{u}_{N,h} \boldsymbol{v}_h = (f, v_h)_{\mathcal{T}^m}, \tag{5.1}$$

for all $v_h \in U_h$. Here $\mathcal{B}_m^N(\partial_t)\boldsymbol{\gamma}_m u_{N,h}$ defined as in (3.15b). Alternatively, we can write it in the following form: find $\mathbf{u}_N \in C^1([0,\, T]; \mathbb{R}^{N_s})$, s.t. $\mathbf{u_N}(.,0) = \partial_t \mathbf{u_N}(.,0) = 0$ and

$$\begin{aligned} &\mathbf{M}\partial_t^2 \mathbf{u}_N + \mathbf{K}\mathbf{u}_N + \mathbf{P}^T \mathbf{W}_m \mathbf{D}_m \left\langle \frac{\boldsymbol{\mu}}{\boldsymbol{\alpha}} \right\rangle \boldsymbol{\Lambda}(0) \mathbf{P}\mathbf{u}_N \\ &+ \mathbf{P}^T \mathbf{W}_m \mathbf{D_m} \sum_{k=0}^{p-1} \sum_{i=0}^{N-1} a_i \frac{\mu_k}{\alpha_k} \partial_t \left(\boldsymbol{\lambda}_{i,k}^N \right) = \mathbf{M}\boldsymbol{f}^n, \\ &\partial_t^2 \boldsymbol{\lambda}_{i,k}^N + \alpha_k^{-1} \omega_n^2 \mathbf{D}_m^2 \boldsymbol{\lambda}_{i,k}^N = \mathbf{P}\mathbf{u}_N, \qquad \boldsymbol{\lambda}_{i,k}^N(0) = \partial_t \boldsymbol{\lambda}_{i,k}^N = 0. \end{aligned} \tag{5.2}$$

Stability. The stability of the formulation (5.1) under the CFL condition for non-weighted 1D wave equation, discretized with the P_1 finite elements and an explicit leap-frog scheme, is rather easy to show, and can be obtained exactly like in Theorem 3.6, see also [9].

5.1.2. *Discretization in Time.* Let us describe how we discretize the approximate problem (3.15a). To obtain a stable discretization, the main idea is to use the explicit **leapfrog** discretization for the volumic terms, and the implicit **trapezoid rule** discretization of the boundary terms. First, however, we introduce some notation. Provided Δt be a time step, let u^n be an approximation to $u(., n\Delta t)$. Let, additionally:

$$\begin{aligned} &D_{\Delta t} v^n = \frac{v^{n+1} - v^{n-1}}{2\Delta t}, \qquad D_{\Delta t}^2 v^n = \frac{v^{n+1} - 2v^n + v^{n-1}}{(\Delta t)^2}, \\ &\{v^n\}_{1/4} = \frac{v^{n+1} + 2v^n + v^{n-1}}{4}, \qquad v^{n+1/2} = \frac{v^n + v^{n+1}}{2}. \end{aligned} \tag{5.3}$$

Formulation. The discretization of (3.15a) reads: given $\mathbf{u}^0 = 0$, $\mathbf{u}^1 = 0 \in \mathbb{R}^{N_s}$, find $(\mathbf{u}^n)_{n=0}^{\infty} \subset \mathbb{R}^{N_s}$, s.t.

$$\mathbf{M}D^2_{\Delta t}\mathbf{u}^n_N + \mathbf{K}\mathbf{u}^n_N + \mathbf{P}^T\Big\langle\frac{\boldsymbol{\mu}}{\boldsymbol{\alpha}}\Big\rangle\boldsymbol{\Lambda}(0)\mathbf{W}_m\mathbf{D}_m\mathbf{P}\{\mathbf{u}^n_N\}_{1/4} + \mathbf{P}^T\mathbf{W}_m\mathbf{D}_m\sum_{k=0}^{p-1}\sum_{i=1}^{N} a_i\frac{\mu_k}{\alpha_k}D_{\Delta t}\left(\boldsymbol{\lambda}^N_{i,k}\right)^n = \mathbf{M}\mathbf{f}^n, \tag{5.4a}$$

$$D^2_{\Delta t}\left(\boldsymbol{\lambda}^N_{i,k}\right)^n + \alpha_k^{-1}\omega_i^2\mathbf{D}_m^2\left\{\left(\boldsymbol{\lambda}^N_{i,k}\right)^n\right\}_{1/4} = D_{\Delta t}\mathbf{P}\mathbf{u}^n_N, \tag{5.4b}$$

$$\left(\boldsymbol{\lambda}^N_{i,k}\right)^0 = \left(\boldsymbol{\lambda}^N_{i,k}\right)^1 = 0. \tag{5.4c}$$

Stability. The formulation (5.4a) is stable under the classical CFL condition

$$C_{CFL} = \left(\frac{\Delta t}{2}\right)^2\rho(\mathbf{M}^{-1/2}\mathbf{K}\mathbf{M}^{-1/2})^{-1} < 1, \tag{5.5}$$

where $\rho(A)$ is the spectral radius of a matrix A. This condition ensures that E_N defined in Theorem 5.1 is an energy. With the notation $\langle\mathbf{v},\mathbf{q}\rangle_A = \langle A\mathbf{v},\mathbf{q}\rangle$, $\|\mathbf{v}\|_A^2 = \langle\mathbf{v},\mathbf{v}\rangle_A$, the stability result reads

Theorem 5.1 (Stability of (5.4))**.** *Let $\mathbf{u}_N$ solve (5.4) with $\mathbf{u}^0 = \mathbf{u}^1 = 0$, and let (5.5) hold true. Then the energy*

$$\begin{aligned}
E_N^{n+1/2} &= \frac{1}{2}\left(\left\|\frac{\mathbf{u}^{n+1}_N - \mathbf{u}^n_N}{\Delta t}\right\|^2_{\mathbf{M}} - \left(\frac{\Delta t}{2}\right)^2\left\|\frac{\mathbf{u}^{n+1}_N - \mathbf{u}^n_N}{\Delta t}\right\|^2_{\mathbf{K}}\right)\\
&\quad + \frac{1}{2}\left\|\mathbf{u}_N^{n+\frac12}\right\|^2_{\mathbf{K}} + \frac{1}{2}\Big\langle\frac{\boldsymbol{\mu}}{\boldsymbol{\alpha}}\Big\rangle\boldsymbol{\Lambda}(0)\|\mathbf{P}u^{n+\frac12}\|^2_{\mathbf{W}_m\mathbf{D}_m}\\
&\quad + \sum_{i=1}^{N} a_i\sum_{k=0}^{p-1}\frac{\mu_k}{\alpha_k}\left(E^N_{i,k}\right)^{n+\frac12},\\
\left(E^N_{i,k}\right)^{n+\frac12} &= \frac{1}{2}\left\|\frac{(\boldsymbol{\lambda}^N_{i,k})^{n+1} - (\boldsymbol{\lambda}^N_{i,k})^n}{\Delta t}\right\|^2_{\mathbf{W}_m\mathbf{D}_m} + \frac{\alpha_k^{-1}\omega_i^2}{2}\left\|\mathbf{D}_m(\boldsymbol{\lambda}^N_{i,k})^{n+\frac12}\right\|^2_{\mathbf{W}_m\mathbf{D}_m},
\end{aligned}$$

satisfies the following stability bound:

$$\sqrt{E_m^{n+1/2}} \le C\Delta t\sum_{k=1}^{n}\|\boldsymbol{f}^k\|_{\mathbf{M}},$$

where C depends on $\boldsymbol{\alpha},\boldsymbol{\mu}$ only.

Proof. The result is obtained by testing the equation (5.4a) with $D_{\Delta t}\mathbf{u}^n$. The only 'non-classical' terms are related to $\boldsymbol{\lambda}$, and can be handled using (5.4b)

$$\begin{aligned}
&\left(\mathbf{W}_m\mathbf{D}_{\mathbf{m}}D_{\Delta t}\left(\boldsymbol{\lambda}^N_{i,k}\right)^n, D_{\Delta t}\mathbf{P}u^n_N\right) = \left(\mathbf{W}_m\mathbf{D}_{\mathbf{m}}D_{\Delta t}\left(\boldsymbol{\lambda}^N_{i,k}\right)^n, D^2_{\Delta t}\left(\boldsymbol{\lambda}^N_{i,k}\right)^n\right)\\
&+ \left(\mathbf{W}_m\mathbf{D}_{\mathbf{m}}D_{\Delta t}\left(\boldsymbol{\lambda}^N_{i,k}\right)^n, \alpha_k^{-1}\omega_i^2\mathbf{D}_m^2\left\{\left(\boldsymbol{\lambda}^N_{i,k}\right)^n\right\}_{1/4}\right).
\end{aligned}$$

The above yields :

$$E_N^{n+\frac12} - E_N^{n-\frac12} = \Delta t\left\langle\mathbf{f}^n, \frac{\mathbf{u}^{n+1} - \mathbf{u}^{n-1}}{\Delta t}\right\rangle_{\mathbf{M}},$$

which can be bounded using the Gronwall's inequality. □ □

Remark 5.2. As discussed in [9], the CFL condition (5.5) coincides with the CFL condition for a P_1-discretization of a non-weighted wave equation.

5.1.3. *Remarks on convergence.* Like for the case of the convolution quadrature discretization in [9], it is not difficult to demonstrate that the resulting discrete scheme is second order in time and first order in space, when measuring the error in the energy norm, with the constants depending on the computational time T polynomially and on some $W^{\ell,1}(0,T;\mathrm{L}^2_\mu(\mathcal{T}^m))$-norm of f. Let us remark as well that the convergence estimates can be shown to be independent of N. Since the proof is very classical, we will not provide the respective result here.

5.2. **Error control in practice.** In practice, to choose the number of poles in the approximation of Λ^N, we do not use the estimates of Theorem 4.5, but rather estimate numerically the quantity

$$r_N = \sum_{n=N+1}^{\infty} \frac{a_n}{\omega_n^2},$$

which controls the approximation error, cf. Theorem 3.7. Remark that, with (3.5),

$$\frac{d^2\mathbf{\Lambda}}{d\omega^2}(0) = -2\sum_{n=0}^{\infty} \frac{a_n}{\omega_n^2}.$$

On the other hand, by Lemma 5.5 and Corollary 5.6 in [10], the above quantity is given by one of the expressions below:

(1) when $\left\langle \frac{\boldsymbol{\mu}}{\boldsymbol{\alpha}} \right\rangle \leq 1$, $\mathbf{\Lambda}''_{\mathfrak{n}}(0) = \mathbf{\Lambda}''_{\mathfrak{d}}(0) = -\left(1 - \langle \boldsymbol{\mu}\boldsymbol{\alpha} \rangle\right)^{-1}$

(2) when $\langle \boldsymbol{\mu}\boldsymbol{\alpha} \rangle < 1 < \left\langle \frac{\boldsymbol{\mu}}{\boldsymbol{\alpha}} \right\rangle$,

$$\mathbf{\Lambda}''_{\mathfrak{n}}(0) = \left(1 - \langle \boldsymbol{\mu}\boldsymbol{\alpha} \rangle\right)^{-1}$$

and

$$\mathbf{\Lambda}''_{\mathfrak{d}}(0) = -\frac{1}{3}\left(\left\langle \frac{\boldsymbol{\mu}}{\boldsymbol{\alpha}} \right\rangle^2 + \left\langle \frac{\boldsymbol{\mu}}{\boldsymbol{\alpha}} \right\rangle + 1\right)\left(\left\langle \frac{\boldsymbol{\mu}}{\boldsymbol{\alpha}} \right\rangle^2 - \langle \boldsymbol{\mu}\boldsymbol{\alpha} \rangle\right)^{-1}.$$

(3) when $\langle \boldsymbol{\mu}\boldsymbol{\alpha} \rangle \geq 1$,

$$\mathbf{\Lambda}''_{\mathfrak{n}}(0) = \mathbf{\Lambda}''_{\mathfrak{d}}(0) = -\frac{1}{3}\left(\left\langle \frac{\boldsymbol{\mu}}{\boldsymbol{\alpha}} \right\rangle^2 + \left\langle \frac{\boldsymbol{\mu}}{\boldsymbol{\alpha}} \right\rangle + 1\right)\left(\left\langle \frac{\boldsymbol{\mu}}{\boldsymbol{\alpha}} \right\rangle^2 - \langle \boldsymbol{\mu}\boldsymbol{\alpha} \rangle\right)^{-1}.$$

Hence, provided N first numerically computed $\tilde{a}_\ell$ and $\tilde{\omega}_\ell$, we estimate r_N as follows:

$$r_N \approx \frac{1}{2}\left(\mathbf{\Lambda}''(0) + 2\sum_{n=1}^{N} \frac{\tilde{a}_n}{\tilde{\omega}_n^2}\right),$$

with $\mathbf{\Lambda}''(0)$ being provided by one of the above expressions.

5.3. **Computing poles and zeros in the approximation $\mathbf{\Lambda}^N_{\mathfrak{a}}$.** In order to use the approximation (3.13), (3.10), it is necessary to evaluate ω_n^2, the poles of $\mathbf{\Lambda}$, and the respective (scaled) residues a_n.

There are several difficulties associated to this problem:

- the location of poles is, in general, not known (and the direct use of the argument principle to estimate the number of poles on a given interval does not seem to be possible, because the poles and zeros of $\mathbf{\Lambda}(\omega)$ interlace, and thus evaluation of the argument principle integral $(2\pi i)^{-1}\int_\gamma \mathbf{\Lambda}'(z)(\mathbf{\Lambda}(z))^{-1}dz$ always results in ± 1 or 0).
- the poles may be located quite close to each other (which poses difficulties in choosing the integration contour to evaluate the residues).
- evaluation of $\mathbf{\Lambda}(\omega)$ close to the real axis may be inaccurate, because of the proximity to the poles.

To overcome (at least) some of these difficulties, we suggest to use an alternative strategy, described in the following sections.

5.3.1. *An auxiliary function.* Let us introduce an auxiliary function

$$\boldsymbol{g}(\omega) := \left(-\omega^{-1}\mathbf{\Lambda}(\omega) - i\right)\left(-\omega^{-1}\mathbf{\Lambda}(\omega) + i\right)^{-1}. \tag{5.6}$$

The following holds true for $\boldsymbol{g}(\omega)$.

Lemma 5.3. *The function $\boldsymbol{g}(\omega)$ is meromorphic in $\mathbb{C}$. Moreover,*

- $|\boldsymbol{g}(\omega)| = 1$ *when* $\omega \in \mathbb{R}$;
- $\boldsymbol{g}(\omega_0) = 1$ *iff either* $\omega_0 = 0$ *or* ω_0 *is a pole of* $\mathbf{\Lambda}(\omega)$.
- *the respective coefficient* a_ℓ, *cf.* (3.5), *is given by* $a_\ell = 4i(\boldsymbol{g}'(\omega_\ell))^{-1}$.

Proof. The proof of the first two conditions is simple and thus we leave it to the reader; as for the computation of a_ℓ, we use the following property:

$$\boldsymbol{g}'(\omega) = -\frac{2i\left(\omega^{-1}\mathbf{\Lambda}(\omega)\right)'}{(-\omega^{-1}\mathbf{\Lambda}(\omega)+i)^2},$$

which, after evaluation in the pole $\omega = \omega_\ell$ gives

$$\lim_{\omega\to\omega_\ell}\boldsymbol{g}'(\omega) = -\lim_{\omega\to\omega_\ell}\frac{2i\left(\omega^{-1}\mathbf{\Lambda}(\omega)\right)'(\omega^2-\omega_\ell^2)^2}{(-\omega^{-1}\mathbf{\Lambda}(\omega)+i)^2(\omega^2-\omega_\ell^2)^2} = \lim_{\omega\to\omega_\ell}\frac{4ia_\ell\omega_\ell^2}{(-a_\ell\omega^2+i(\omega^2-\omega_\ell)^2)^2},$$

and hence the result. □

Thus, to find the poles of $\mathbf{\Lambda}(\omega)$ it suffices to find $\omega \in \mathbb{R}\setminus\{0\}$, s.t. $\boldsymbol{g}(\omega) = 1$, and to find a_ℓ we can compute the derivatives in this points.

5.3.2. *Remarks on the evaluation of $g(\omega)$ in one point.* To evaluate $\boldsymbol{g}(\omega)$, we use the same ideas as in [9] for the evaluation of $\mathbf{\Lambda}(\omega)$. For this we will write an equation similar to (3.5), satisfied by $\boldsymbol{g}(\omega)$. Re-expressing $\mathbf{\Lambda}(\omega)$ via $\boldsymbol{g}(\omega)$,

$$-\omega^{-1}\mathbf{\Lambda}(\omega) = i\frac{1+\boldsymbol{g}(\omega)}{1-\boldsymbol{g}(\omega)},$$

and replacing $\mathbf{\Lambda}$ in (3.5) by the above expression, after some computations we obtain

$$\begin{aligned}\boldsymbol{g}(\omega) &= \frac{\boldsymbol{G}(\omega)\tan\omega + i\boldsymbol{g}_{\alpha,\mu}(\omega) - i\boldsymbol{G}(\omega) + \boldsymbol{g}_{\alpha,\mu}(\omega)\tan\omega}{\boldsymbol{G}(\omega)\tan\omega + i\boldsymbol{g}_{\alpha,\mu}(\omega) + i\boldsymbol{G}(\omega) - \boldsymbol{g}_{\alpha,\mu}(\omega)\tan\omega}\\ &= \frac{\boldsymbol{g}_{\alpha,\mu}(\omega) - \boldsymbol{G}(\omega)\mathrm{e}^{2i\omega}}{\boldsymbol{G}(\omega) - \boldsymbol{g}_{\alpha,\mu}(\omega)\mathrm{e}^{2i\omega}},\end{aligned} \tag{5.7}$$

where

$$\boldsymbol{G}(\omega) := \prod_{j=0}^{p-1}(1-\boldsymbol{g}(\alpha_j\omega)), \qquad \boldsymbol{g}_{\alpha,\mu}(\omega) = \sum_{j=0}^{p-1}\mu_j(1+\boldsymbol{g}(\alpha_j\omega))\prod_{k\neq j}(1-\boldsymbol{g}(\alpha_k\omega)).$$

This expression resembles (3.5), in the sense that knowing $\boldsymbol{g}(z)$ for $|z| < |\boldsymbol{\alpha}|_\infty|\omega|$ allows to evaluate $\boldsymbol{g}(\omega)$. Thus, to compute $\boldsymbol{g}(\omega)$, we can employ the same algorithm as we used to compute $\boldsymbol{\Lambda}(\omega)$ in [9]. Let us remark that the use of this method requires additionally that $\boldsymbol{g}(\omega)$ be analytic in the vicinity of $\omega = 0$ (which is true because $\boldsymbol{g}(\omega)$ is meromorphic and continuous in $\omega = 0$), as well as a method to evaluate $\boldsymbol{g}(\omega)$ for small frequencies ($|\omega| < r$, for some fixed parameter of the algorithm $r > 0$), e.g. via a truncated Taylor expansion. The Taylor coefficients of expansion of $\boldsymbol{g}(\omega)$ in $\omega = 0$ can be easily expressed via known Taylor coefficients for $\boldsymbol{\Lambda}(\omega)$, cf. [10, Appendix C], and (5.6).

Remark 5.4. The computation of the Taylor coefficients of $\boldsymbol{g}$ of large orders may suffer from roundoff errors (because of the substractions/additions of the Taylor coefficients of $\boldsymbol{\Lambda}(\omega)$, which can be large); however, we did not notice any numerical problems caused by this (provided that the frequencies ω for which $\boldsymbol{g}$ is approximated by its Taylor expansion are small enough).

Alternatively, one can approximate $\boldsymbol{\Lambda}(\omega)$ for small frequencies ω via its truncated Taylor expansion, and then use (5.6) to express $\boldsymbol{g}(\omega)$.

Remark 5.5. For fixed $r > 0$ and the number N of Taylor coefficients used for evaluation of $\boldsymbol{g}(\omega)$ for $|\omega| < r$, the complexity of the algorithm scales as $O(\log^{p+1}|\omega|)$ with $|\omega| \to +\infty$, cf. [9].

5.3.3. *Computing poles and residues of* $\boldsymbol{\Lambda}(\omega)$. In order to compute the poles of $\boldsymbol{\Lambda}(\omega)$ on $[0, L]$, we subdivide $[0, L]$ in sufficiently small intervals and interpolate $\boldsymbol{g}(\omega)$ on each of this intervals using Chebyshev interpolation. This piecewise-Chebyshev interpolant is referred to as $\boldsymbol{g}_c(\omega)$.

Next, we proceed as per Lemma 5.3: we compute zeros of z_k of a polynomial interpolant $\operatorname{Im}\boldsymbol{g}_c(\omega)$, and check whether $|\operatorname{Re}\boldsymbol{g}_c(z_k) - 1| < \varepsilon$, for a given ε. If this is the case, z_k is a pole of $\boldsymbol{\Lambda}(\omega)$.

Evaluation of the coefficients a_ℓ is done via differentiation of the polynomial $\boldsymbol{g}_c$.

Remark 5.6. The reason why we subdivide the original interval $[0, L]$ into multiple intervals and interpolate $\boldsymbol{g}(\omega)$ on the intervals lies in the behaviour of $\boldsymbol{g}(\omega)$: despite the fact that this function is smooth, it may oscillate rapidly (depending on the values $\boldsymbol{\alpha}$, $\boldsymbol{\mu}$), and hence require polynomial interpolation of high degree. An illustration to this is shown in Figure 6.

Moreover, to ensure a sufficient accuracy of the polynomial interpolation, at each subinterval we check whether $\max_\omega ||\boldsymbol{g}(\omega)| - 1| > \varepsilon_{tol}$ for a given ε_{tol}: when this is the case, the subinterval is subdivided into several subintervals, and $\boldsymbol{g}$ is interpolated on this subinterval; this is done recursively.

An actual implementation of the algorithm was done with the help of Chebfun [22, 21, 4].

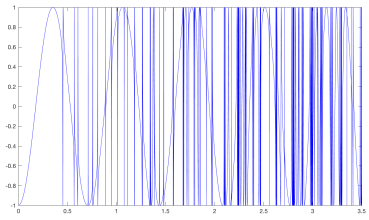

FIGURE 6. Dependence of $\operatorname{Re} \boldsymbol{g}(\omega)$ on ω for the Neumann problem, with $\boldsymbol{\alpha} = (0.8, 0.75)$ and $\boldsymbol{\mu} = (0.5, 0.5)$

5.4. **Numerical Results.** All the experiments of this section are performed on the reference tree (i.e. $\mu_{0,0} = 1$ and the length of the root branch $\ell_{0,0} = 1$). Moreover, we use the scheme (5.4a-5.4c) with the mass-lamped finite elements (thus all the norms are computed with the help of the mass-lamped matrices).

5.4.1. *Validity of the method.* To validate the correctness of the approach, we compare it to the convolution quadrature approximation of the transparent boundary conditions, cf. [9]. In particular, we truncate the tree to $m = 3$ generations, and compute the solution on the tree $\mathcal{T}^{m-1}$ with the help of the N-term transparent boundary conditions. The reference solution u_{ref} is computed on the truncated tree $\mathcal{T}^m$ (i.e. the tree with 4 generations), with the help of the CQ method, with the same discretization parameters.

We solve the Dirichlet problem for $\boldsymbol{\alpha} = (0.3, 0.6)$, $\boldsymbol{\mu} = (0.5, 1)$. As a source we take the function supported on the root edge of the tree

$$f(s,t) = 10^5 \exp(-\sigma(s-0.5)^2 - \sigma(t-0.5)^2)(s-0.5), \quad \sigma = 10^3.$$

In all the cases we choose the discretization with $h = 10^{-4}$ and $\Delta t \approx 9.9 \cdot 10^{-5}$. The above function is approximately band-limited in time with the maximal frequency in its Fourier transform being $\omega_{max} \approx 107$ (we cut-off at 10^{-5}-accuracy). This implies that the maximal frequency present in the Fourier transform of (2.9) is roughly $\omega_{max} |\boldsymbol{\alpha}|_\infty^m \approx 0.6^3 \cdot 107 \approx 23$. This means that N should be chosen large enough to ensure that all the poles inside the interval $(0, 23)$ are included into the approximation (3.13), i.e. $N \geq 27$. A more precise error control is achieved by computing the value r_N as described in Section 5.2. In particular,

$$r_{100} \approx 9 \cdot 10^{-3}, \quad r_{250} \approx 4.1 \cdot 10^{-3}, \quad r_{500} \approx 2.2 \cdot 10^{-3}, \quad r_{950} \approx 1.2 \cdot 10^{-3}.$$

We choose these values of N to verify the validity of the method. Denoting by u_N the numerical solution obtained from using the approximation of the transparent boundary conditions (3.13), we plot the dependence of the error

$$e_N^n = \frac{\|u_N^n - u_{ref}^n\|_{\mathrm{L}^2_\mu(\mathcal{T}^{m-1})}}{\max_\ell \|u_{ref}^\ell\|_{\mathrm{L}^2_\mu(\mathcal{T}^{m-1})}}, \tag{5.8}$$

on time $n\Delta t$ in Figure 7. The dependence of the solution u_N on time evaluated in one point of the tree is shown in Figure 8.

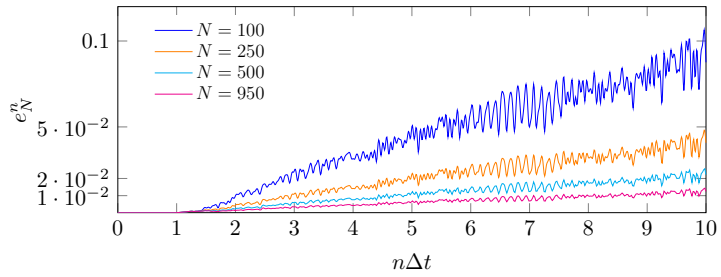

FIGURE 7. Dependence of the error e_N^n defined in (5.8) on time $n\Delta t$ for different values of the truncation parameter N.

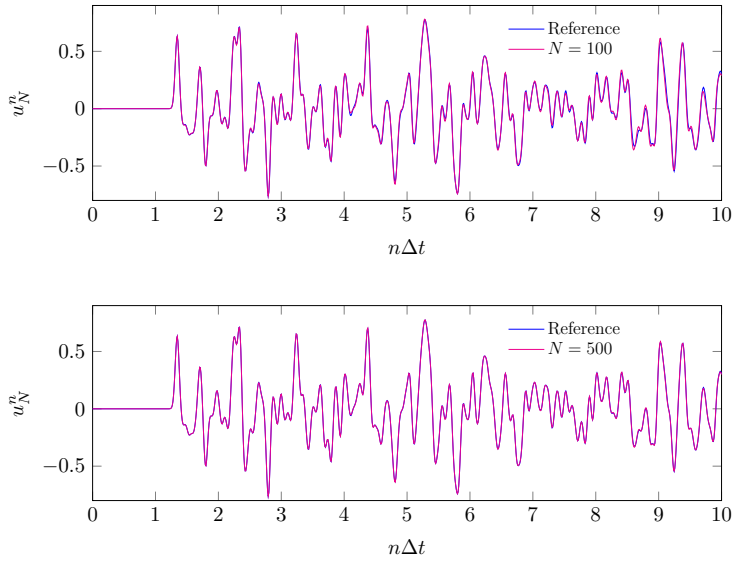

FIGURE 8. Top: dependence of the solution u_N^n measured in the middle of the edge $\Sigma_{2,0}$ of the tree on time $n\Delta t$. Top: $N = 100$, bottom: $N = 500$

5.4.2. *Convergence rates.* In this section we study the convergence rates of the method, according to the results of Theorem 3.7 and Theorem 4.5.

For this we conduct four numerical experiments, which cover all three cases of Theorem 4.5. We compute the solution u_N to the Neumann problem on a truncated tree $\mathcal{T}^{m-1}$, with $m = 3$, with the help of the approximated transparent boundary conditions (3.13), for different values of N, and compare it to the reference solution u_{ref} computed with the help of the convolution quadrature method [9] on the truncated tree $\mathcal{T}^{m-1}$. In all the experiments we use the discretization with the spatial step $h = 10^{-4}$ and the time step $\Delta t = 9.9 \cdot 10^{-5}$. As a source term we take

a function supported on the root branch of the tree

$$f(s,t) = 10^5 \exp(-\sigma(s-0.5)^2 - \sigma(t-0.5)^2)(s-0.5), \quad \sigma = 100.$$

All the computations are done on the time interval $(0,T)$, with $T = 10$, divided into N_t time steps. We measure the dependence of the following relative error on the order N of the transparent boundary conditions:

$$e^N_{rel} := \frac{e^N_{abs}}{\max\limits_{\ell=0,\dots,N_t} \|u^\ell_{ref}\|_{\mathrm{L}^2_\mu(\mathcal{T}^{m-1})}}, \quad e^N_{abs} = \max_{\ell=0,\dots,N_t} \|u^\ell_N - u^\ell_{ref}\|_{\mathrm{L}^2_\mu(\mathcal{T}^{m-1})}. \tag{5.9}$$

We compare the quantity e^N_{rel} to the quantity r_N, computed numerically as described in Section 5.2, as well as a theoretical upper bound given in Theorem 4.5. The results are given in Figures 9, 10. In these figures we observe in particular that the numerically computed value r_N provides an excellent estimate for the convergence rates, as expected, and can be potentially used as an error estimator.

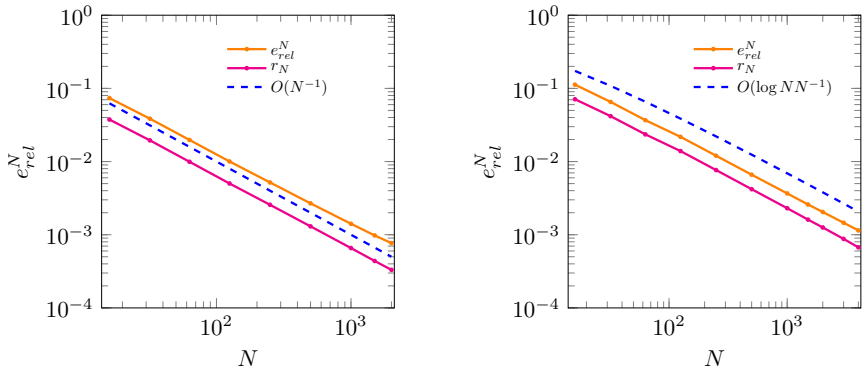

FIGURE 9. Relative error (5.9) depending on N. Left: $\boldsymbol{\alpha} = (0.2, 0.5)$, $\boldsymbol{\mu} = (0.6, 0.1)$ ($d_s < 1$, with $r_N = O(N^{-1})$). Right: $\boldsymbol{\alpha} = (0.7, 0.3)$, $\boldsymbol{\mu} = (0.3, 0.6)$ ($d_s = 1$, with $r_N = O(N^{-1}\log N)$).

As a complement to Figures 9, 10, we present the numerically estimated order of convergence associated to different experiments in Table 1. We observe a rather good agreement with the theoretical convergence estimates, especially in the cases $\boldsymbol{\alpha} = (0.7, 0.3)$ and $\boldsymbol{\alpha} = (0.7, 0.6)$. In the case $\boldsymbol{\alpha} = (0.5, 0.65)$, the convergence rates measured from the numerical errors are very close to the convergence rates measured for the values r_N (the absolute error between the measured convergence rates does not exceed $3.5 \cdot 10^{-2}$). Most likely this is related to the fact that in this case the asymptotic regime has not been reached for the range of N considered.

Finally, in the case $\boldsymbol{\alpha} = (0.2, 0.5)$, we remark that the convergence order deteriorates slightly. Because there exists a discrepancy between the convergence rates measured from the numerical error and the convergence rates measured for the numerically computed value r_N (where it is very close to 1), we think that it is likely to be related to the accuracy of computation of the poles and residues in the method.

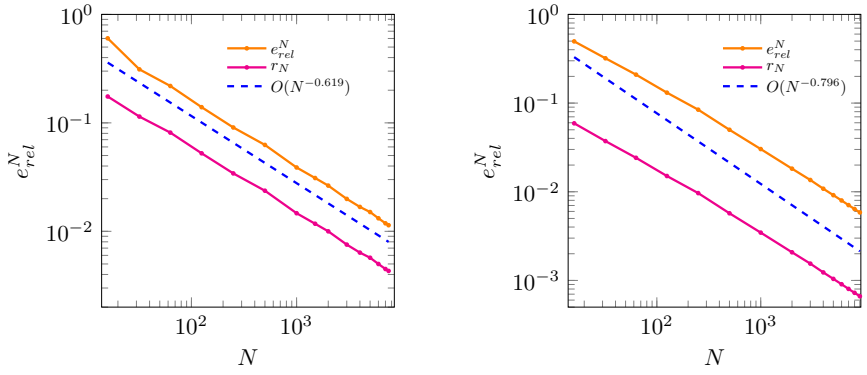

FIGURE 10. Relative error (5.9) depending on N. Left: $\boldsymbol{\alpha} = (0.7, 0.6)$, $\boldsymbol{\mu} = (0.3, 0.6)$ ($d_s \approx 1.615$, $r_N = O(N^{-\frac{1}{d_s}})$). Right: $\boldsymbol{\alpha} = (0.5, 0.65)$, $\boldsymbol{\mu} = (2, 1)$ ($d_s \approx 1.256$, $r_N = O(N^{-\frac{1}{d_s}})$). In this latter case the Dirichlet and Neumann problems coincide.

Value of N	Numerical convergence rate d in different experiments			
N_k	$\boldsymbol{\alpha} = (0.2, 0.5)$	$\boldsymbol{\alpha} = (0.7, 0.3)$	$\boldsymbol{\alpha} = (0.7, 0.6)$	$\boldsymbol{\alpha} = (0.5, 0.65)$
16	-	-	-	-
32	0.94	1.15	0.95	0.63
63	0.99	1.15	0.52	0.63
125	0.99	0.99	0.66	0.68
250	0.95	1.1	0.62	0.64
500	0.95	1.0	0.53	0.75
1000	0.93	1.0	0.69	0.72
2000	0.88	0.98	0.56	0.73
4000	-	0.96	0.65	0.75
7000	-	-	0.62	0.76
Theoretical d	1	1	0.62	0.796

TABLE 1. Numerically measured convergence rates in different experiments. In the particular case of $\boldsymbol{\alpha} = (0.7, 0.3)$ (where the convergence is $O(N^{-1} \log N)$), the quantity provided in the above table is defined as

$$d = \frac{\log\left(e^{N_{k+1}}_{rel} / e^{N_k}_{rel}\right)}{\log\left(N^{-1}_{k+1} \log N_{k+1} / (N^{-1}_k \log N_k)\right)}.$$

6. Conclusions and Open Questions

In this work, we have constructed transparent boundary conditions for the weighted wave equation on a self-similar one-dimensional fractal tree. The approach presented here is alternative to the convolution quadrature [9] and is based

on the truncation of the meromorphic series representing the symbol of the DtN operator. The complexity of the method depends on the number of poles in the truncated series; we have presented estimates on the number of poles, required to achieve a desired accuracy ε (which, in the best case, is $O(\varepsilon^{-1})$). While the convergence in term of the number of poles is rather slow, one of the advantages of this method is that its cost does not increase with time (unlike the convolution quadrature approach). Our future efforts are directed towards improving the convergence of the technique, based on approximation of the remainder of the meromorphic series.

Acknowledgements

We are grateful to Adrien Semin (TU Darmstadt, Germany) for providing his code NETWAVES, and to Konstantin Pankrashkin (University Paris-Sud, Orsay, France) for many fruitful discussions.

References

1. The Audible Human Project of acoustics and vibrations laboratory of University of Illinois at Chicago, 2007-2014.
2. Patricia Alonso-Ruiz, Daniel J. Kelleher, and Alexander Teplyaev, Energy and Laplacian on Hanoi-type fractal quantum graphs, J. Phys. A **49** (2016), no. 16, 165206, 36. MR 3479135
3. A. H. Barnett and A. Hassell, Boundary quasi-orthogonality and sharp inclusion bounds for large Dirichlet eigenvalues, SIAM J. Numer. Anal. **49** (2011), no. 3, 1046–1063. MR 2812557
4. Zachary Battles and Lloyd N. Trefethen, An extension of MATLAB to continuous functions and operators, SIAM J. Sci. Comput. **25** (2004), no. 5, 1743–1770. MR 2087334
5. Maxence Cassier, Patrick Joly, and Maryna Kachanovska, Mathematical models for dispersive electromagnetic waves: an overview, Comput. Math. Appl. **74** (2017), no. 11, 2792–2830. MR 3725831
6. Bjorn Engquist and Andrew Majda, Absorbing boundary conditions for the numerical simulation of waves, Math. Comp. **31** (1977), no. 139, 629–651. MR 0436612
7. William Feller, An introduction to probability theory and its applications. Vol. II, John Wiley & Sons, Inc., New York-London-Sydney, 1966. MR 0210154
8. Céline Grandmont, Bertrand Maury, and Nicolas Meunier, A viscoelastic model with non-local damping application to the human lungs, M2AN Math. Model. Numer. Anal. **40** (2006), no. 1, 201–224. MR 2223510
9. Patrick Joly and Maryna Kachanovska, Transparent boundary conditions for wave propagation in fractal trees: convolution quadrature approach, submitted, August 2019.
10. Patrick Joly, Maryna Kachanovska, and Adrien Semin, Wave propagation in fractal trees. Mathematical and numerical issues, Netw. Heterog. Media **14** (2019), no. 2, 205–264. MR 3959344
11. Patrick Joly and Adrien Semin, Construction and analysis of improved Kirchoff conditions for acoustic wave propagation in a junction of thin slots, Paris-Sud Working Group on Modelling and Scientific Computing 2007–2008, ESAIM Proc., vol. 25, EDP Sci., Les Ulis, 2008, pp. 44–67. MR 2521686
12. Naotaka Kajino, Spectral asymptotics for Laplacians on self-similar sets, J. Funct. Anal. **258** (2010), no. 4, 1310–1360. MR 2565841
13. Jun Kigami, Analysis on fractals, Cambridge Tracts in Mathematics, vol. 143, Cambridge University Press, Cambridge, 2001. MR 1840042
14. Jun Kigami and Michel L. Lapidus, Weyl's problem for the spectral distribution of Laplacians on p.c.f. self-similar fractals, Comm. Math. Phys. **158** (1993), no. 1, 93–125. MR 1243717
15. I. Lasiecka, J.-L. Lions, and R. Triggiani, Nonhomogeneous boundary value problems for second order hyperbolic operators, J. Math. Pures Appl. (9) **65** (1986), no. 2, 149–192. MR 867669

16. Michael Levitin and Dmitri Vassiliev, Spectral asymptotics, renewal theorem, and the Berry conjecture for a class of fractals, Proc. London Math. Soc. (3) **72** (1996), no. 1, 188–214. MR 1357092
17. Bertrand Maury, The respiratory system in equations, Springer-Verlag, 2013.
18. Bertrand Maury, Delphine Salort, and Christine Vannier, Trace theorems for trees, application to the human lungs, Network and Heteregeneous Media **4** (2009), no. 3, 469 – 500.
19. T. J. Royston, X. Zhang, H. A. Mansy, and R. H. Sandler, Modeling sound transmission through the pulmonary system and chest with application to diagnosis of a collapsed lung, The Journal of the Acoustical Society of America **111** (2002), no. 4, 1931–1946.
20. Adrien Semin, Propagation d'ondes dans des jonctions de fentes minces, Ph.D. thesis, 2010.
21. Lloyd N. Trefethen, Computing numerically with functions instead of numbers, Math. Comput. Sci. **1** (2007), no. 1, 9–19. MR 2384813
22. ———, Approximation theory and approximation practice, Society for Industrial and Applied Mathematics (SIAM), Philadelphia, PA, 2013. MR 3012510

Appendix A. Proof of Lemma 3.8

The proof relies on an inequality from the proof of Theorem 3.24 of [10]. It was established (remark that $\int\limits_{\Gamma_m} \boldsymbol{\mu\alpha}|\boldsymbol{v}|^2 = \|\Pi v\|^2_{\mathrm{L}^2_\mu(\mathcal{G}^m)}$ in the notation of [10]) that

$$\int\limits_{\Gamma_m} \boldsymbol{\mu\alpha}|\boldsymbol{v}|^2 \le C_m \|\partial_s v\|^2_{\mathrm{L}^2_\mu(\mathcal{T}^m)}, \quad C_m = \begin{cases} m^2 \big\langle \boldsymbol{\mu\alpha} \big\rangle^m & \text{if } \big\langle \boldsymbol{\mu\alpha} \big\rangle = |\boldsymbol{\alpha}|^2_\infty, \\ m|\boldsymbol{\alpha}|^2_\infty \dfrac{\big\langle \boldsymbol{\mu\alpha} \big\rangle^m - |\boldsymbol{\alpha}|^{2m}_\infty}{\big\langle \boldsymbol{\mu\alpha} \big\rangle - |\boldsymbol{\alpha}|^2_\infty}, & \text{if } \big\langle \boldsymbol{\mu\alpha} \big\rangle \ne |\boldsymbol{\alpha}|^2_\infty. \end{cases}$$

It is not difficult to verify that $C_m \le Cm^2 \max(\big\langle \boldsymbol{\mu\alpha} \big\rangle^m, |\boldsymbol{\alpha}|^{2m}_\infty)$, $C > 0$, hence the conclusion.

Appendix B. Proof of Lemma 4.2

All the arguments of [3] are repeated almost verbatim; the only minor modification in [3] is required in the proof of Lemma 2.1, where we choose a smooth multiplier $\chi(s)$ (in the notation of [3], $a(s)$) supported on $\Sigma_{0,0}$, s.t. $\chi(M^*) = -1$.

The proof of the result of Lemma 4.2 relies on the following lemma.

Lemma B.1. *Let $\mathcal{J}_{\omega,\eta} := \{j : |\omega_j - \omega| < \eta\}$, where $\omega \ge 1$, $\eta > 0$. Let $K := \#\mathcal{J}_{\omega,\eta}$. Any $\varphi_c = \sum\limits_{j\in\mathcal{J}_{\omega,\eta}} c_j\varphi_j$, where $\boldsymbol{c} = (c_j)_{j\in\mathcal{J}_{E,\eta}} \in \mathbb{R}^K$ and φ_j ($\equiv \varphi_{\mathfrak{a},j}$) are defined in 3.4, satisfies*

$$|\partial_s \varphi_c(M^*)| \le C_\eta \omega \|\boldsymbol{c}\|_{\mathbb{R}^K}. \tag{B.1}$$

The constant C_η depends only on η and the tree under consideration.

To see why the result of Lemma B.1 implies the bound of Lemma 4.2, it suffices to take $\boldsymbol{c} := (\partial_s \varphi_j(M^*))_{j\in\mathcal{J}_{\omega,\eta}}$. Then (B.1) rewrites

$$\left| \sum_{j\in\mathcal{J}_{\omega,\eta}} (\partial_s \varphi_j(M^*))^2 \right| \le C_\eta \omega \left| \sum_{j\in\mathcal{J}_{\omega,\eta}} (\partial_s \varphi_j(M^*))^2 \right|^{\frac{1}{2}},$$

which results in the following statement:

$$\sum_{j\in\mathcal{J}_{\omega,\eta}} (\partial_s \varphi_j(M^*))^2 \le C_\eta \omega^2.$$

From the above it follows

$$\sum_{j\in\mathcal{J}_{\omega,\eta}} (\partial_s\varphi_j(M^*))^2\omega_j^{-2} \le C_\eta \frac{\omega^2}{|\omega-\eta|^2} \le \widetilde{C}_\eta,$$

for ω sufficiently large. For ω small, the desired bound follows by remarking that $\omega_j \neq 0$ and there is only a finite number of the eigenfrequencies on the interval $(0,\omega)$. This proves Lemma 4.2.

Proof of Lemma B.1. Let χ be a (sufficiently smooth) function supported on the root branch of the tree $\Sigma_{0,0}$, with $\chi(M^*)=1$ and $\chi(M_{0,0})=0$. Without loss of generality, let us assume that the length of the root branch is 1. Then

$$\begin{aligned}\varphi_c'(M^*)^2 &= -\int_0^1 \frac{d}{ds}\left(\chi(s)\varphi_c'(s)\right)^2 \\ &= -\int_0^1 \chi'(s)(\varphi_c'(s))^2 ds - 2\int_0^1 \chi(s)\varphi_c'(s)\varphi_c''(s)ds.\end{aligned} \tag{B.2}$$

Next, let us remark the following properties:

$$\|\varphi_j\| = 1, \quad \|\partial_s\varphi_j\|^2 = \omega_j^2, \quad (\varphi_j,\varphi_k) = (\partial_s\varphi_j,\partial_s\varphi_k) = 0, \ \text{ for } j\neq k, \tag{B.3}$$

$$\|\varphi_c\|_{\mathrm{L}^2_\mu} = \|\boldsymbol{c}\|, \qquad \|\partial_s\varphi_c\|^2 = \sum_{j\in\mathcal{J}_{\omega,\eta}} \omega_j^2 c_j^2 \le (\omega+\eta)^2\|\boldsymbol{c}\|^2. \tag{B.4}$$

The first term in (B.2) thus satisfies

$$I_1 := -\int_0^1 \chi'(s)(\varphi_c'(s))^2 ds \le |\chi'|_\infty(\omega+\eta)^2\|\boldsymbol{c}\|^2. \tag{B.5}$$

The second term can be rewritten as follows

$$I_2 := -2\int_0^1 \chi(s)\varphi_c'(s)\varphi_c''(s)ds = 2\int_0^1 \chi(s)\varphi'(s)\sum_{j\in\mathcal{J}_{\omega,\eta}} \omega_j^2 c_j\varphi_j(s)ds. \tag{B.6}$$

Naively bounding the above term with the Cauchy-Schwartz would result in

$$I_2 \le C\|\varphi'\|\left\|\sum_{j\in\mathcal{J}_{\omega,\eta}} \omega_j^2 c_j\varphi_j\right\| \le C(\omega+\eta)^3\|\boldsymbol{c}\|^2,$$

which is, for $\omega>1$, ω times more than what we would like to have. To overcome this, we will use, on one hand, the fact that ω_j in the above sum are close to ω, and, on the other hand, the orthogonality of eigenfunctions (expressed in particular in the first equation of (B.4)). For $s\in\Sigma_{0,0}$, we rewrite

$$\sum_{j\in\mathcal{J}_{\omega,\eta}} \omega_j^2 c_j\varphi_j(s) = \sum_{j\in\mathcal{J}_{\omega,\eta}} (\omega_j^2-\omega^2)c_j\varphi_j(s) + \omega^2\varphi_c(s) = r_c(s) + \omega^2\varphi_c(s).$$

Then (B.6) gives

$$I_2 = 2\int_0^1 r_c(s)\chi(s)\varphi_c'(s)ds + 2\omega^2\int_0^1 \chi(s)\varphi_c'(s)\varphi_c(s)$$
$$= 2\int_0^1 r_c(s)\chi(s)\varphi_c'(s)ds - \omega^2\int_0^1 \varphi_c^2(s)\chi'(s)ds,$$

where to get the last identity we integrated by parts and used the fact that $\chi(1) = 0$ and $\varphi_c(0) = 0$.

With (B.4), we remark that

$$\|r_c\| \le (2\eta\omega + \eta^2)\|\boldsymbol{c}\|, \tag{B.7}$$

Therefore, by the Cauchy-Schwartz inequality, and the bound (B.4),

$$I_2 \le |\chi|_\infty(2\eta\omega + \eta^2)(\omega + \eta)\|\boldsymbol{c}\|^2 + |\chi'|_\infty\omega^2\|\boldsymbol{c}\|^2.$$

Combining the above bound and (B.5) in (B.2) results in

$$\|\varphi_c'(M^*)\|^2 \le C(\eta)\omega^2\|\boldsymbol{c}\|^2,$$

which proves the statement of the lemma. □

Appendix C. Proof of Lemma 4.4

Preliminary considerations. Before proving the desired lower bound, let us explain the intuition behind the proof. Remark that the eigenfunctions of $-\mu^{-1}\partial_s(\mu^{-1}\partial_s)$ on the root branch of $\mathcal{T}$ are necessarily of the form

$$\varphi_n(s) = C_n \sin\omega_n s, \quad C_n > 0.$$

We can easily relate C_n to the coefficients $a_n = (\partial_s\varphi_n(0))^2\omega_n^{-2}$, cf. (3.5):

$$\varphi_n(s) = \sqrt{a_n}\sin\omega_n s. \tag{C.1}$$

We are thus interested in estimating the quantities

$$Q_{\omega,\eta} := \sum_{\ell:\,|\omega_n-\omega|<\eta} a_n. \tag{C.2}$$

In a particular case when $p = 1$, the tree $\mathcal{T}$ reduces to an interval $(0, L)$. If additionally $\mu = 1$, then the quantities ω_n^2 and φ_n are respectively eigenvalues and eigenfunctions of $-\Delta$ for the Dirichlet/mixed problem (depending on the problem under consideration) on $(0, L)$. In this case, provided that η is sufficiently large, the interval $\{\ell : |\omega_n - \omega| < \eta\}$ represents the band of frequencies that are 'significant' in the decomposition of $\sin\omega s \in L^2(0, L)$ over the basis $\{\varphi_n\}$. More precisely,

$$\text{on } (0,\, L), \quad \sin\omega s = \sum_{n=0}^{\infty}\gamma_n^\omega\varphi_n, \quad \gamma_n^\omega = \int_0^L \sin\omega s\,\varphi_n(s)ds,$$

We can show that

$$\sin\omega s = \sum_{\ell:\,|\omega_n-\omega|<\eta} \gamma_n^\omega \varphi_n + \sum_{\ell:\,|\omega_n-\omega|\geq\eta} \gamma_n^\omega \varphi_n, \qquad \text{where}$$

$$\sup_{\omega\geq 1} \left\| \sum_{\ell:\,|\omega_n-\omega|\geq\eta} \gamma_n^\omega \varphi_n \right\|_{L^2}^2 = \sup_{\omega\geq 1} \sum_{\ell:\,|\omega_n-\omega|\geq\eta} (\gamma_n^\omega)^2 \to 0, \qquad \eta\to\infty.$$

Let us show how the above observation helps in the proof that $Q_{\omega,\eta} > C$, for some η sufficiently large. Evidently, from (C.1),

$$|\gamma_n^\omega| \leq \sqrt{a_n} L. \tag{C.3}$$

Therefore, choosing η sufficiently large, we see that with some $\varepsilon > 0$, it holds for all $\omega > 0$,

$$\|\sin\omega s\|_{L^2}^2 \leq \sum_{\ell:\,|\omega_n-\omega|<\eta} (\gamma_n^\omega)^2 + \varepsilon.$$

For $\omega > L^{-1}$, by a direct computation it follows that $\|\sin\omega s\|_{L^2}^2 > \frac{L}{4}$. Then, for all $\omega > L^{-1}$,

$$\sum_{\ell:\,|\omega_n-\omega|<\eta} (\gamma_n^\omega)^2 \geq \frac{L}{4} - \varepsilon. \tag{C.4}$$

With (C.3), the above gives us a desired inequality on the coefficients a_n:

$$\sum_{\ell:\,|\omega_n-\omega|<\eta} a_n \geq \frac{1}{4L} - \frac{\varepsilon}{L^2}.$$

This non-rigorous reasoning is justified in the proof of Lemma 4.4, where we come back to the case of an arbitrary fractal tree $\mathcal{T}$.

Proof of Lemma 4.4. Step 1. Spectral decomposition of a function that equals to $\sin\omega s$ *on* $\Sigma_{0,0}$. Let us consider the function $v_\omega(s)$, which equals to $\sin\omega s$ on the root branch of the tree, and vanishes otherwise. It belongs to $\mathrm{L}^2_\mu(\mathcal{T})$, and therefore, the following series converges in $\mathrm{L}^2_\mu(\mathcal{T})$:

$$v_\omega = \sum_{n=0}^{\infty} \gamma_n^\omega \varphi_n \equiv \sum_{\omega_n} \gamma_n^\omega \varphi_n = \underbrace{\sum_{|\omega_n-\omega|<\eta} \gamma_n^\omega \varphi_n}_{v^s_{\omega,\eta}} + \underbrace{\sum_{|\omega_n-\omega|\geq\eta} \gamma_n^\omega \varphi_n}_{v^i_{\omega,\eta}}. \tag{C.5}$$

The indices s and i in $v^{s,i}_{\omega,\eta}$ stand for 'significant' and 'insignificant'.

Step 2. Proving that $\sup_{\omega\geq 1} \|v^i_{\omega,\eta}\|_{\mathrm{L}^2_\mu(\mathcal{T})} \to 0$ *as* $\eta\to\infty$. Let us demonstrate that

$$\|v^i_{\omega,\eta}\|^2_{\mathrm{L}^2_\mu(\mathcal{T})} \equiv \sum_{|\omega_n-\omega|\geq\eta} |\gamma_n^\omega|^2$$

can be bounded independently of ω, by a quantity that depends on η. For this, let us compute

$$\gamma_n^\omega = \int_{\mathcal{T}} v_\omega(s)\varphi_n(s)\mu ds \overset{(C.1)}{=} \sqrt{a_n}\int_0^1 \sin(\omega s)\sin(\omega_n s)ds \tag{C.6}$$

$$= \sqrt{a_n}\,\frac{\omega_n \sin\omega\cos\omega_n - \omega\cos\omega\sin\omega_n}{\omega^2-\omega_n^2}. \tag{C.7}$$

From (C.6) we see that $|\gamma_n^\omega| < \sqrt{a_n}$; combining this with (C.7), we obtain

$$|\gamma_n^\omega| \le \sqrt{a_n}\,\min\left(\frac{1}{|\omega-\omega_n|},1\right). \tag{C.8}$$

Next, to bound $v^i_{\omega,\eta}$, let us assume without loss of generality that $\omega = W \in \mathbb{N}$ and $\eta = k \in \mathbb{N}$:

$$\begin{aligned}\|v^i_{W,k}\|^2_{\mathrm{L}^2_\mu(\mathcal{T})} &= \sum_{|\omega_n - W|\ge k} |\gamma_n^\omega|^2 = \sum_{\omega_n \le W-k} |\gamma_n^\omega|^2 + \sum_{\omega_n \ge W+k} |\gamma_n^\omega|^2 \\ &\overset{(C.8)}{\le} \sum_{\omega_n\le W-k} \frac{a_n}{(W-\omega_n)^2} + \sum_{\omega_n\ge W+k}\frac{a_n}{(\omega_n - W)^2}. \end{aligned}\tag{C.9}$$

To bound each of the above terms, we will make use of Lemma 4.2. The first term in (C.9) vanishes when $W < k$; otherwise, it can be rewritten as follows:

$$\begin{aligned}\sum_{\omega_n\le W-k}\frac{a_n}{(W-\omega_n)^2} &= \sum_{\ell=0}^{W-k-1}\sum_{\ell\le\omega_n<\ell+1}\frac{a_n}{(W-\omega_n)^2} \\ &\le \sum_{\ell=0}^{W-k-1}\frac{1}{(W-\ell-1)^2}\sum_{\ell\le\omega_n<\ell+1} a_n.\end{aligned}$$

Using Lemma 4.2, we obtain the following bound, for some $C>0$:

$$\sum_{\omega_n\le W-k}\frac{a_n}{(W-\omega_n)^2} \le C\sum_{\ell=0}^{W-k-1}\frac{1}{(W-\ell-1)^2} = C\sum_{\ell=k}^{W-1}\frac{1}{\ell^2} \le \frac{C_1}{k}, \tag{C.10}$$

where C_1 does not depend on W.

It remains to bound the second term in (C.9); we use the same ideas:

$$\begin{aligned}\sum_{\omega_n\ge W+k}\frac{a_n}{(\omega_n-W)^2} &= \sum_{\ell=W+k}^{\infty}\sum_{\ell\le\omega_n<\ell+1}\frac{a_n}{(\omega_n-W)^2} \\ &\le \sum_{\ell=W+k}^{\infty}\frac{1}{(\ell-W)^2}\sum_{\ell\le\omega_n<\ell+1} a_n \le C\sum_{\ell=W+k}^{\infty}\frac{1}{(\ell-W)^2},\end{aligned}$$

where the last bound again follows from Lemma 4.2. We thus easily obtain the uniform in W bound

$$\sum_{\omega_n\ge W+k}\frac{a_n}{(\omega_n-W)^2} < \frac{C_2}{k}. \tag{C.11}$$

Combining (C.10) and (C.11) into (C.9), and noting that the above considerations extend easily to the case $\omega, \eta \notin \mathbb{N}$, we finally obtain the desired bound

$$\sup_{\omega \geq 1} \|v^i_{\omega,\eta}\|^2 \leq \frac{C}{\eta}, \quad C > 0. \tag{C.12}$$

Step 3. Relating $\|v^s_{\omega,\eta}\|_{\mathrm{L}^2_\mu(\mathcal{T})}$ *and* $\sum_{k:\,|\omega_n-\omega|<\eta} a_n$. An upper bound for $\|v^s_{\omega,\eta}\|$ can be obtained from (C.8):

$$\|v^s_{\omega,\eta}\|^2_{\mathrm{L}^2_\mu(\mathcal{T})} \equiv \sum_{n:\,|\omega_n-\omega|<\eta} |\gamma^\omega_n|^2 \leq \sum_{k:\,|\omega_n-\omega|<\eta} a_n. \tag{C.13}$$

Step 4. Lower bound for $\sum_{k:\,|\omega_n-\omega|<\eta} a_n$. The equation (C.5) together with (C.12) and (C.13) implies

$$\|v_\omega\|^2_{\mathrm{L}^2_\mu(\mathcal{T})} = \|v^s_{\omega,\eta}\|^2_{\mathrm{L}^2_\mu(\mathcal{T})} + \|v^i_{\omega,\eta}\|^2_{\mathrm{L}^2_\mu(\mathcal{T})} \leq \sum_{k:\,|\omega_n-L|<\eta} a_n + C\eta^{-1}. \tag{C.14}$$

On the other hand, a direct computation gives

$$\|v_\omega\|^2_{\mathrm{L}^2_\mu(\mathcal{T})} = \frac{1}{2} - \frac{\sin(2\omega)}{4\omega}, \quad \text{thus } \|v_\omega\|^2_{\mathrm{L}^2_\mu(\mathcal{T})} \geq \frac{1}{4} \text{ for } \omega \geq 1 \tag{C.15}$$

(recall that $\omega \geq 1$ is in the assumption of the Lemma).

Let us choose $\eta > 0$ large enough, so that $C\eta^{-1} < \frac{1}{8}$. Then (C.14) and (C.15) rewrite

$$\sum_{k:\,|\omega_n-\omega|<\eta} a_n \geq \frac{1}{8}.$$

We have thus proven the desired statement. □

POEMS (INRIA-CNRS-ENSTA), ENSTA ParisTech, 828 Boulevard des Maréchaux, 91120 Palaiseau France

E-mail address: patrick.joly@inria.fr

POEMS (INRIA-CNRS-ENSTA), ENSTA ParisTech, 828 Boulevard des Maréchaux, 91120 Palaiseau France

E-mail address: maryna.kachanovska@inria.fr